Co-expressed subunits of dual genetic origin define a conserved supercomplex mediating essential protein import into chloroplasts

Silvia Ramundo [1,2], Yukari Asakura [3], Patrice A. Salomé [4], Daniela Strenkert [4,5], Morgane Boone [1], Luke C. M. Mackinder [6], Kazuaki Takafuji [7], Emine Dinc [8], Michèle Rahire[8], Michèle Crèvecoeur [8], Leonardo Magneschi [9], Olivier Schaad [10], Michael Hippler [9,11], Martin C. Jonikas [12,2], Sabeeha Merchant [4,5], Masato Nakai [3,13], Jean-David Rochaix [8,13] and Peter Walter [1,2.13]

[1] Department of Biochemistry and Biophysics, University of California at San Francisco, San Francisco, USA
[2] Howard Hughes Medical Institute
[3] Laboratory of Organelle Biology, Institute for Protein Research, Osaka University, Osaka, Japan
[4] Department of Chemistry and Biochemistry, UCLA, Los Angeles, USA
[5] Present address: QB3, University of California, Berkeley, USA
[6] Department of Biology, University of York, UK
[7] Graduate School of Medicine, Osaka University, Osaka, Japan
[8] Departments of Molecular Biology and Plant Biology, University of Geneva, Geneva, Switzerland
[9] Institute of Plant Biology and Biotechnology, University of Münster, Münster, Germany
[10] Department of Biochemistry, University of Geneva, Geneva, Switzerland
[11] Institute of Plant Science and Resources, Okayama University, Kurashiki, Japan
[12] Department of Molecular Biology, Princeton University, USA
[13] Corresponding authors: Nakai@protein.osaka-u.ac.jp; Jean-David.Rochaix@unige.ch; Peter@walterlab.ucsf.edu

Abstract

In photosynthetic eukaryotes, thousands of proteins are translated in the cytosol and imported into the chloroplast through the concerted action of two translocons — termed TOC and TIC — located in the outer and inner membranes of the chloroplast envelope, respectively. The degree to which the molecular composition of the TOC and TIC complexes is conserved over phylogenetic distances has remained controversial. Here, we combine transcriptomic, biochemical, and genetic tools in the green alga Chlamydomonas (*Chlamydomonas reinhardtii*) to demonstrate that, despite a lack of evident sequence conservation for some of its components, the algal TIC complex mirrors the molecular composition of a TIC complex from *Arabidopsis thaliana.* The Chlamydomonas TIC complex contains three nuclear-encoded subunits, Tic20, Tic56 and Tic100, and one chloroplast-encoded subunit, Tic214, and interacts with the TOC complex, as well as with several uncharacterized proteins to form a stable supercomplex (TicToc), indicating that protein import across both envelope membranes is mechanistically coupled. Expression of the nuclear and chloroplast genes encoding both known and the here newly identified TicToc components is highly coordinated, suggesting that a mechanism for regulating its biogenesis across compartmental boundaries must exist. Conditional repression of Tic214, the only chloroplast-encoded subunit in the TicToc complex, impairs the import of chloroplast proteins with essential roles in chloroplast ribosome biogenesis and protein folding and induces a pleiotropic stress response, including several proteins involved in the chloroplast unfolded protein response. These findings underscore the functional importance of the TicToc supercomplex in maintaining chloroplast proteostasis.

Introduction

Chloroplasts are vital organelles in eukaryotic photosynthetic organisms. Akin to mitochondria, they are thought to have arisen from an endosymbiotic event, in which a cyanobacterial ancestor was engulfed by a eukaryotic cell (*1*). Over time, most cyanobacterial genes were transferred to the nuclear genome of the host, which nowadays supplies the organelle with the majority of its resident proteins from the cytosol. An essential step in the establishment of chloroplasts was the evolution of the translocons that select chloroplast precursor proteins synthesized in the cytosol and import them through protein-conducting channels into the chloroplast. The translocons are multiprotein complexes, located in the outer and inner chloroplast envelope membranes. Receptor proteins intrinsic to the translocons recognize a signal-peptide (for chloroplasts and mitochondria also called transit-peptide) at the N-terminus of chloroplast precursor proteins that is cleaved off and quickly degraded upon import [original findings: (*2-12*); recent reviews: (*13-19*)]. Based on the membrane in which the translocons reside, they are referred to as translocon of the outer and inner chloroplast membrane (TOC and TIC), respectively (*20*).

To date, the vast majority of the translocon components have been identified and characterized through biochemical studies in green peas (*Pisum sativum*) (*8, 21-30*) and genetic studies in Arabidopsis (*Arabidopsis thaliana*) (*11, 29, 31-37*). Their evolutionary conservation in other photosynthetic eukaryotes has been inferred from phylogenetic sequence alignments (*15*). The molecular composition of the TOC complex is relatively well understood. It consists of three core subunits, namely the pre-protein receptors Toc159 and Toc34, and the protein-conducting channel, Toc75 (*11, 38-41*). By contrast, the molecular identity and function of the subunits in the TIC complex is still under debate. Earlier studies performed on pea chloroplasts revealed several of its subunits, including Tic110, Tic62, Tic55, Tic40, Tic32, Tic22, and Tic20 (*21, 24-28*). However, there is no consensus as to which components form the protein-conducting channel: while multiple studies demonstrated a channel activity for Tic20 *in vitro* (*42-45*), it is still debated whether Tic110 is also directly involved in forming a channel (*46-49*). The scenario has been further complicated by the recent isolation of a

novel large TIC complex in Arabidopsis, termed the "1-MDa complex" (*42, 44*), that contains Tic20 in association with a different set of proteins, namely Tic100, Tic56 and Tic214. Tic214 is unique in that it is the only known translocon component encoded by the chloroplast genome (*44*). The 1-MDa TIC complex associates with translocating pre-proteins, displays pre-protein-dependent channel activity (*44*), and functionally and physically cooperates with the Ycf2/Ftshi complex, a recently-identified ATP-driven import motor (*50*). However, two recent studies reported that chloroplast protein import is only partially impaired in Arabidopsis mutants lacking Tic56 (*51*), as well as in Arabidopsis plants in which Tic214 was down-regulated to undetectable levels upon treatment with spectinomycin, a drug that selectively inhibits chloroplast and mitochondrial translation (*52*). Furthermore, no clear orthologue for Tic214 has been identified in grasses, glaucophytes, red algae, or some dicots (*52-55*). Hence, published work raises skepticism whether the 1-MDa TIC complex in general, and Tic214 in particular, are functionally important during chloroplast protein import.

Here, we address these questions using multipronged and unbiased approaches. Using co-immunoprecipitation analyses and co-expression studies, we demonstrate that in Chlamydomonas, all the subunits of the Arabidopsis 1-MDa TIC complex are conserved and are part of a supercomplex that contains all known TOC subunits, as well as several novel subunits. Furthermore, we show that the supercomplex is functional *in vitro* and *in vivo*, and is vital to maintain chloroplast proteostasis.

Results

The molecular architecture of plant TOC and TIC is conserved in algae.

To establish a comprehensive inventory of TIC and TOC components in Chlamydomonas, we first used the Arabidopsis TOC and TIC protein sequences and queried the Chlamydomonas proteome using the Basic Local Alignment Search Tool (BLAST) algorithm (*56*) (*SI Appendix*, Tables S1 and S2). We identified single putative Chlamydomonas orthologs for most Arabidopsis TOC components, as well as some TIC

components. Because genes with similar functions are more likely to be co-expressed than random genes (*57-59*), we calculated their associated Pearson's correlation coefficients (PCC) as a measure of transcriptional correlation (Fig. 1). We used the 26S proteasome as a control for a strong positive correlation (Fig. 1 *A* and *C*) (*59*). A pairwise comparison of all Chlamydomonas genes provided a control for lack of correlation (Fig. 1*C*, *SI Appendix*, Table S3). The analysis was based on RNAseq data from 518 samples derived from 58 independent experiments (for more details, see Materials and Methods). A positive PCC value indicates that two genes are co-expressed, a PCC value close to zero indicates no correlation, while a negative PCC value indicates that two genes have opposite expression patterns. We arranged genes in groups by hierarchical clustering to display their co-expression relationships (Fig. 1 *A* and *B*) (*SI Appendix*, Table S3). By comparison to the proteasome, the overall correlation of translocon components considered in this analysis is relatively weak (*SI Appendix*, Table S4).

Nevertheless, we found that Chlamydomonas chloroplast translocon genes can be classified in two clusters, hereafter referred to as *cpA* and *cpB* (Fig. 1 *B* and *C*) (*SI Appendix*, Table S3). The most strongly correlated genes in c*pA* include *TOC120*, *TOC90*, *TOC75*, *TIC110*, *TIC20*, previously shown to be essential for protein import in Arabidopsis (*11, 29, 30*). Except for *TOC64*, the much less correlated genes in *cpB* encode paralogs of genes in *cpA*. We surmise that the subgroup distribution may indicate a functional separation of components that are essential core translocon components (*cpA*) from those that may be dispensable or specialized (*cpB*). We obtained very similar results when performing an identical analysis with Arabidopsis plastid translocon genes (*SI Appendix,* Fig. S1), recapitulating previously reported expression patterns (*60*).

The BLAST searches identified all known subunits of the Chlamydomonas TOC complex (*SI Appendix*, Table S2). By contrast, similar BLAST searches failed to uncover all Chlamydomonas orthologs for the recently characterized components of the Arabidopsis TIC complex, except for *TIC20,* yet Chlamydomonas orthologs for Tic56

and Tic214 were previously proposed (*44*). Thus, to determine the composition of the Chlamydomonas TIC complex, we tagged Chlamydomonas Tic20 with a C-terminal yellow fluorescent protein (YFP) and a triple FLAG epitope (*61*) and carried out an immunopurification assay under native conditions, followed by mass-spectrometric analysis.

This strategy identified three Tic20-interacting proteins (Table 1, *SI Appendix*, Table S6), whose structural domain organization is similar to that of Arabidopsis Tic56, Tic100, and Tic214, respectively (*SI Appendix*, Fig. S2). Following the Arabidopsis naming convention, we will refer to these proteins as Chlamydomonas Tic56, Tic100, and Tic214. Tic56 and Tic100 are encoded by the nuclear genes Cre17.g727100 and Cre06.g300550, respectively, while Tic 214 is encoded by the essential chloroplast gene *orf1995* (*62*), hereafter referred to as *tic214*.

Remarkably, several other proteins also co-immunoprecipitated with Tic20, including orthologs of the Arabidopsis TOC: Toc90 (Cre17.g734300), Toc120 (Cre17.g707500), Toc75 (Cre03.g175200) and Toc34 (Cre06.g252200) (Table 1). These findings suggest that the Chlamydomonas TIC and TOC complexes form a stable supercomplex (here referred to as TicToc) that spans the outer and inner chloroplast membranes, as previously shown in land plants (*9, 25, 63*).

We next performed a reciprocal co-immunoprecipitation followed by mass-spectrometry, using Tic214 as bait to confirm that the TicToc supercomplex indeed comprises chloroplast-encoded Tic214. Since the chloroplast genome can be manipulated with relative ease by homologous recombination in Chlamydomonas (*64*), we inserted three copies of the HA tag into the endogenous *tic214* locus (*SI Appendix*, Fig. S3*A*). Immunoblot analysis using an anti-HA antibody or an antibody raised against Tic214 detected a protein of smaller size than expected (around 110 kDa, hereafter referred to as Tic214*) (*SI Appendix*, Fig. S3*B*). Nevertheless, we retrieved peptides covering most of the Tic214 protein sequence upon affinity purification (*SI Appendix*, Fig. S3 *C* and *D*, Table S7). This result confirms that Tic214 is translated over the entire

gene length and suggests that its abnormal electrophoretic mobility arises from at least one proteolytic nick, which may be introduced in the cell or during sample preparation, resulting in two or more stable fragments that remain part of the complex.

As expected from its role as bait in the immunoprecipitation, Tic214 emerged as the protein with the highest number of spectral counts (Table 1, *SI Appendix*, Table S7). Importantly, the analysis confirmed that Tic214 interacts with the same TOC subunits found in association with Tic20: namely Toc34, Toc75, and Toc90 (Table 1). We did not detect peptides derived from Tic20 or Tic56, likely because their electrophoretic mobility overlap with those of the antibody chains migrating in gel regions that were excluded from the analysis.

Taken together, these results suggest that the molecular architecture of the TOC and TIC complexes of land plants are conserved in chlorophyte algae, despite the lack of strong enough sequence similarity of some of its components that would have allowed their detection by BLAST analysis. Moreover, the ability of TIC and TOC to form a TicToc supercomplex, as well as the presence of a single chloroplast-encoded protein (Tic214), are phylogenetically conserved.

Several novel proteins associate with the TicToc supercomplex.

Aside from the known TOC and TIC subunits discussed above, we identified several uncharacterized proteins in our pull-downs using Tic20 (*SI Appendix*, Table S6) and Tic214 (*SI Appendix*, Table S7) as bait. The overlapping set of proteins found in both pull-downs contained three FtsH-like AAA proteins (Fhl1, Fhl3, and an uncharacterized FtsH-like protein encoded by Cre17.g739752, that we named Ctap1 for chloroplast translocon associated protein 1). These three proteins lack the zinc-binding motif that is critical for the catalytic activity of typical FtsH metalloproteases; in this respect, they strongly resemble the Arabidopsis FtsHi proteins that were recently shown to associate with translocating pre-proteins during *in vitro* import reactions and serve as ATP-driven import motors (*50*). The immunoprecipitations also identified six additional previously uncharacterized proteins (Ctap2-7; encoded by Cre16.g696000,

Cre12.g532100, Cre17.g722750, Cre03.g164700, Cre04.g217800 and Cre08.g378750, respectively) (Table 1, *SI Appendix*, Tables S6 and S7) that co-purified with both Tic20 and Tic214. Ctap2 is a 150 kDa protein that contains a C-terminal domain with homology to UDP-N-acetylglucosamine-pyrophosphorylases, while Ctap3-7 have no recognizable sequence motifs.

Fhl1, Ctap1, and Ctap5 bear predicted chloroplast transit peptides according to the chloroplast localization prediction software Predalgo (*65*), and Fhl3 and Ctap6 contain predicted transmembrane regions that may anchor them in the chloroplast envelope. A recently published genome-wide algal mutant library (*66*) does not contain any insertional mutants that would disrupt the coding region of any of these uncharacterized genes, hinting that these genes may be essential.

The expression of TicToc components is coordinated across compartmental boundaries.

As an extension of the approach described in Fig. 1, we surmised that if the newly identified proteins in the Tic20 and Tic214 pull-downs represented genuine components of the TicToc supercomplex, their encoding genes likewise might be co-expressed. To test this hypothesis, we recalculated the PCC correlation matrix after the addition of these genes to our original list of chloroplast translocon components (Fig. 2). Indeed, all genes coding for the proteins that co-purified with Tic20 and Tic214 exhibited correlated expression, as shown in Fig. 2 *A* and *C* (group *cp2*) (*SI Appendix*, Table S4).

Based on these results, we next extended the co-expression analysis to look for other genes that correlate in their expression with *TIC20*. In this way, we identified 25 additional genes exhibiting co-expression with *TIC20* (*SI Appendix*, Table S8), (group *cp3,* Fig. 2 *A-C*). Since proteins encoded by *cp3* genes were not identified in the pull-downs, we hypothesize that they may be involved in the regulation/assembly of the translocon, or be more loosely associated and washed off during affinity purification. We did not further pursue these proteins in this investigation.

Because the vast majority of the expression datasets used in our analyses are based on polyA-selected RNA samples, they do not include mRNAs transcribed inside an organelle where polyA addition does not occur. Thus, to test for co-expression between *tic214* and nucleus-encoded TIC and TOC genes, we used a dataset that was generated by random priming and interrogated nuclear and chloroplast gene expression changes over the diurnal cycle (12 h dark / 12 h light regime) (*67*). We observed that the expression profile of *tic214* followed that of the nucleus-encoded TIC and TOC components closely, with peaks in the early dark and light phases (Fig. 3*A*). The expression of *tic214* also correlated with that of *orf2971*, a yet uncharacterized chloroplast gene. *orf2971* encodes a protein that resembles Ycf2, the chloroplast-encoded subunit of the Ycf2/FtsHi protein import motor recently identified in Arabidopsis (*50*). Orf2971 was identified during the Tic20 pull-down (*SI Appendix*, Table S6).

A similar expression pattern was also observed for the chloroplast *rpo* genes (encoding the chloroplast RNA polymerase subunits) and *orf528*, another chloroplast gene of unknown function (*68*) (Fig. 3*B*). Although unexpected, these correlations are specific, as we observed no correlation between the expression profiles of *tic214* and that of most other chloroplast genes, including those involved in photosynthesis and ribosome biogenesis, such as *psaB* and *rps12,* which thus serve as negative controls (Fig. 3*C*).

Taken together, the results of the Tic20 and Tic214 co-immunoprecipitation, combined with co-expression analysis, paint a comprehensive picture of translocon composition that strongly supports the assignment of the newly identified proteins as *bona fide* subunits and/or potential biogenesis factors and regulators of the TicToc supercomplex Chlamydomonas. Moreover, our analysis points to an extensive control network(s) that coordinates their expression across compartmental boundaries and over the diurnal cycle.

The TicToc supercomplex is stable.

To assess the stability of the TicToc supercomplex, we affinity-purified the Tic20-tagged complex and analyzed it by blue native polyacrylamide gel electrophoresis (PAGE), followed by SDS- (2D blue native/SDS-PAGE). We found that the proteins associated with Tic20 co-migrate as a large complex (Fig. 4 *A* and *B*). These spots were not detected by silver staining when the affinity purification was performed using extracts derived from an untagged strain (*SI Appendix*, Fig. S4*A*). Mass-spectrometry of discrete protein spots derived from the large complex identified Tic56 and Tic214, as well as Toc34, Toc75, Toc90, Ctap2, Ctap4 and Ctap5. Moreover, we obtained independent confirmation about the presence of Tic214, Tic20, Tic56 and Tic100 by targeted immunoblot analysis with antibodies raised against each protein (Fig. 4*B*, *SI Appendix*, Fig. S4*B*).

As a control, we solubilized the TicToc supercomplex from chloroplast membranes derived from a strain lacking the Tic20-tagged protein. Immunoblot analysis after 2D blue native/SDS-PAGE revealed that Tic20, Tic56, Tic100, and Tic214 all migrated as part of the large complex (Fig. 4*C*), demonstrating that the presence of a FLAG-tag has no impact on the formation or composition of the TicToc supercomplex.

Next, we repeated the Tic20-FLAG affinity purification from membrane extracts prepared with different non-ionic detergents: digitonin, dodecylmaltoside (DDM), and Triton X-100. Immunoblotting analysis after 2D blue native/SDS-PAGE (Fig. 4*D*) detected the four TIC complex components (Tic20, Tic56, Tic100, and Tic214), following membrane solubilization with all detergents, confirming these proteins as core components of the chloroplast translocon. By contrast, Ctap2 was only found with Tic20 in the presence of digitonin, but not with DDM or Triton X-100 (Fig. 4*D*), suggesting that its association is detergent-sensitive.

The TicToc supercomplex functionally associates with chloroplast pre-proteins.

To validate that the TicToc supercomplex functions in importing chloroplast-targeted proteins, we produced two small pre-proteins in *E. coli*: pre-Rubisco small

subunit Rbcs2 and pre-ferredoxin Fdx1, bearing purification tags and TEV protease cleavage sites (Fig. 5*A*). We then incubated the purified pre-proteins with intact Chlamydomonas chloroplasts in the presence of ATP (0.3 or 3 mM) to initiate the import reaction. After a 15 min incubation, we collected chloroplasts and any bound pre-proteins ("Tot" in Fig. 5*B*) by centrifugation. An aliquot of the enriched chloroplast fraction was subjected to freeze-thaw cycles to extract fully imported proteins from the stroma ("Sup" in Fig. 5*B*). For both pre-proteins, we detected the precursor and the mature cleaved protein in the Tot fraction, whereas the stromal fraction (Sup) was enriched with mature cleaved proteins. In the case of pre-Fdx1, all import events (binding of precursor, translocation, and maturation) were dependent on externally added ATP (Fig. 5*B*); for pre-Rbcs2, we observed mature size proteins in the Sup fraction even in the absence of added ATP, possibly mediated by residual ATP contained in the isolated chloroplasts (Fig. 5*B*).

To confirm the ATP dependence of pre-protein translocation into the stroma, we used the protease thermolysin (*69*), which degrades proteins associated with the outer chloroplast membrane, but cannot access those translocated into the stroma. In this assay, the addition of ATP was required for complete translocation and maturation for both pre-Rbcs2 and pre-Fdx1 (Fig. 5*C*, *SI Appendix*, Fig. S5).

To identify the TIC and TOC components that are juxtaposed to the pre-proteins during import, we isolated chloroplasts at the end of an import reaction carried out with or without ATP addition. We then solubilized membrane fractions with digitonin and purified translocation intermediates through the protein A tag by affinity chromatography on IgG Sepharose followed by TEV-mediated elution under non-denaturing condition as depicted in Fig. 5*D*. As a negative control, we omitted the pre-incubation step with protein A-tagged precursors. When probing the eluted fractions with antibodies against TIC complex components Tic20, Tic56, Tic100, and Tic214, we found that the association of all TIC proteins was stimulated by ATP (Fig. 5*E*), consistent with an energized translocation event even for pre-RbcS2. Ctap2 was among the proteins

identified in the eluted fractions (Fig. 5*E*), providing further evidence of its potential role in pre-protein import.

We confirmed these results by unbiased mass spectrometry of the immunoprecipitated complexes. In the case of the Fdx1 precursor translocation intermediate, several TIC and TOC proteins were enriched in the purified fraction in an ATP-dependent manner. Notably, Tic214 and Ctap2 topped the list with the highest spectral counts detected in the presence of ATP (*SI Appendix*, Fig. S6 *A* and *B*), followed by other proteins identified above (Table 2). The same proteins also associated with pre-Rbcs2. However, in this case, the spectral counts were comparable in the presence or absence of ATP (*SI Appendix*, Table S9). This result is consistent with the *in vitro* import assays shown in Fig. 5 *B* and *E*.

Taken together, our results show that the components of the TicToc supercomplex, identified by bioinformatics, protein pull-downs, co-expression analysis, are indeed part of an import-competent machinery.

tic214 expression is required for normal chloroplast morphology and proteostasis.

To assess the role of *tic214 in vivo*, we engineered a strain (Y14) that allows conditional repression of this chloroplast gene in the presence of vitamins (vitamin B_{12} and thiamine, hereafter referred to as "Vit") (Fig. 6*A*, *SI Appendix*, Fig. S7) (*70-72*). As a control, we used the parental strain (A31), in which the addition of Vit does not affect *tic214* expression. As expected for an essential gene, Vit addition to the medium blocked the growth of Y14 cells but not of A31 control cells (Fig. 6 *B* and C). Immunoblot analysis confirmed a time-dependent decrease in the level of Tic214* (Fig. 6*D*). This result further validated that Tic214* originates from *tic214*.

To further characterize the consequences of Tic214 depletion, we visualized cells by transmission electron microscopy. As shown in Fig. 6*E*, *tic214* repression caused a massive cellular swelling and resulted in a chloroplast with highly

disorganized thylakoid ultrastructure and accumulation of starch granules, both typical traits of cells experiencing chloroplast proteotoxic stress (*71, 73, 74*). In agreement with this observation, we found that the time-dependent decrease in Tic214 inversely correlates with the induction of Vipp2 (Fig. 6*D*), a marker of the chloroplast unfolded protein response (cpUPR) (*71, 75*). The cpUPR is a stress-induced signaling network that responds to impairment of chloroplast proteostasis to maintain organellar health (*71, 73, 76-79*).

tic214 repression impairs protein import into chloroplasts.

If Tic214 is a *bona fide* and essential component of the chloroplast translocon, its depletion should block protein import. To obtain direct evidence for translocation defects, we aimed to detect an accumulation of non-translocated chloroplast pre-proteins. To this end, we used tandem mass spectrometric analysis of protein extracts from strain Y14 collected following Tic214 repression and compared the results to the A31 control strain (*SI Appendix*, Table S10). Since unimported chloroplast proteins are quickly degraded by the cytosolic ubiquitin-26S proteasome system (*16, 80, 81*), we incubated each culture with the proteasome inhibitor MG132 before sampling. We limited our analysis to those proteins for which at least ten peptides could be identified in one of the six conditions used in the experiment (2, 4, and 6 days; -/+Vit). This arbitrary cut-off narrowed the dataset to 1,458 of the 5,105 proteins detected, of which 1,427 are encoded by nuclear genes, and 427 are predicted to be chloroplast-localized (*SI Appendix*, Table S11). Among these, we identified 44 proteins for which we detected sequences derived from their predicted transit peptides only upon Tic214 repression (Fig. 7 *A* and *B*, *SI Appendix*, Table S11), indicating that their translocation into the chloroplast was impaired. Some of the peptides included the transit peptide cleavage site, suggesting that they were derived from pre-proteins that did not access the stromal presequence protease (*82, 83*). In addition, seven of these proteins were acetylated at their N-terminal methionine, and five were ubiquitylated only upon Tic214 repression (*SI Appendix*, Table S11). Together, the presence of peptides containing chloroplast transit peptide sequences, the accumulation of uncleaved pre-proteins, and the detection of two post-translational modifications observed only in cytosolic proteins

(*36, 84*), strongly suggests that the import of these chloroplast proteins is impaired in the absence of Tic214.

A manually-curated functional annotation of these 44 proteins revealed that they are involved in various metabolic pathways, including some important reactions such as amino acid synthesis, purine synthesis, one-carbon metabolism, protein folding/degradation, ribosome biogenesis and translation, and photosynthesis (Fig. 7 *B* and *C* and *SI Appendix*, Tables S11 and S12). These data suggest that the import of some chloroplast proteins with essential functions in chloroplast protein folding and ribosome biogenesis requires Tic214, thus explaining why Tic214 depletion causes chloroplast proteotoxicity, inducing the cpUPR. A recent study identified a set of 875 chloroplast stress-responsive proteins (*75*). Although we only detected 91 of these proteins by mass spectrometry here, a vast majority (78 out of 91) was upregulated upon Tic214 depletion, and the expression of 45 of the encoding genes is dependent on Mars1, a critical component of cpUPR signaling (*SI Appendix*, Fig. S8 and Table S13) (*75*).

Discussion

Despite the universal importance of chloroplasts in sustaining life on Earth, there is surprisingly little consensus regarding the molecular machineries that carry out protein import into these organelles. Here, we demonstrate that all of the subunits of the 1-MDa TIC complex previously identified in Arabidopsis are functionally conserved in Chlamydomonas, indicating that this protein import module has been maintained over approximately 1.1 billion years of evolution (*85*). This conclusion is supported by a combination of gene co-expression, protein-protein interaction, and translocation analyses, yet has previously been controversial because sequence comparison analyses failed to identify orthologs for some components of the complex. Thus, our data show that proteins performing essential functions such as chloroplast protein import can be highly divergent in their primary sequence.

In agreement with their functional conservation, we found that in Chlamydomonas, as in Arabidopsis, the TIC complex interacts with the TOC complex to form a TicToc supercomplex. This supercomplex includes several uncharacterized proteins. In particular, we identified three AAA proteins (Fhl3, Fhl1, and Ctap1) and a potential Ycf2 ortholog, Orf2971, that may act as ATP-driven import motors, as previously shown for Arabidopsis and tobacco (*50*). In addition, we found six other uncharacterized chloroplast translocon-associated proteins (Ctap2-7) in the Chlamydomonas supercomplex that were not identified in Arabidopsis. Their topology, function, and evolutionarily conservation remain to be determined. Analysis of several Chlamydomonas transcriptomic datasets revealed that the expression patterns of genes encoding these newly identified components are highly correlated with known TIC and TOC subunits, supporting the idea that these proteins participate in the same biological process.

Our co-expression analysis uncovered additional nuclear and chloroplast genes encoding proteins that were not identified in co-immunoprecipitation experiments, yet may play a role in chloroplast translocon assembly or regulation. Elucidating the exact function of these genes will provide valuable insights into our understanding of the chloroplast protein import machinery.

Importantly, we found that the co-expression of translocon components is not restricted to nuclear-encoded subunits, for which co-regulation was previously shown in Arabidopsis (*60*), but also encompasses chloroplast-encoded subunits. Indeed, chloroplast *tic214* and *orf2971* are co-expressed with nuclear *TIC20* during the Chlamydomonas diurnal cycle, suggesting their common regulation. Thus, in addition to the photosynthetic complexes and the chloroplast ribosome (*86-88*), the chloroplast translocon emerges as yet another example of coordinated gene expression between the chloroplast and nuclear compartment.

In Arabidopsis, TIC and TOC are linked together through Tic236, an integral inner-membrane protein that directly binds to Toc75 via its C-terminal domain protruding into the intermembrane space (*89*). Although BLAST analyses identify an algal orthologue of Tic236 (Cre05.g243150), we did not detect this protein in our experiments or co-expression studies. Hence, how the TicToc supercomplex of Chlamydomonas is held together remains an open question.

To assess the role of the TicToc supercomplex *in vivo*, we engineered a conditional expression system for Tic214. Upon its depletion, we observed severe effects on chloroplast morphology and cell growth, as well as the induction of cpUPR target proteins. By shot-gun proteomic analysis *in vivo*, we positively identified tens of proteins that retained their chloroplast transit peptides upon Tic214 repression. These pre-proteins were detected in the presence of proteasome inhibitors, unmasking their otherwise transient nature. Since some of these proteins have essential functions, including those involved in chloroplast ribosome biogenesis, our data explain why Tic214 is indispensable for cell survival. Hence, the defect in chloroplast translation, previously observed in an Arabidopsis *tic56* mutant (*90*), is likely due to an indirect consequence of a malfunctioning TicToc supercomplex.

In conclusion, we here demonstrate the power of using Chlamydomonas as a model system to dissect the composition, evolution, and regulation of the chloroplast translocon, and, by extension, of other evolutionarily conserved multiprotein complexes. The outstanding stability of the TicToc supercomplex identified in this study, combined with the ease of growing large amounts of Chlamydomonas cells, now opens unprecedented opportunities for the structural and functional characterization of this essential molecular machinery that firmly rivets the inner and outer chloroplast envelope membranes.

Materials and Methods

Strains, Growth Conditions and Media

Chlamydomonas reinhardtii strains were grown on Tris-acetate phosphate (TAP) or minimal (HSM) solid medium containing 1.5% Bacto-agar (*91, 92*) at 25°C in constant light (60-40 µmol m^{-2} s^{-1}), dim light (10 µmol m^{-2} s^{-1}) or in the dark. Growth medium containing vitamin B_{12} and Thiamine-HCl (Vit) was prepared as previously described (*70*).

Co-expression analysis

We mainly followed the steps outlined by (*93, 94*) to assess gene co-expression and generate *TIC20* co-expression networks. We collected raw reads from 58 independent RNAseq experiments, representing 518 samples, and re-mapped them to version v5.5 of the Chlamydomonas genome. Gene expression estimates, in fragments per kilobase of exon model per million reads mapped (FPKMs), were then normalized in three steps: 1) $\log_2$(FPKM + 1), to account for genes with zero FPKMs; 2) quantile normalization with the R package *preprocessCore*; 3) normalization by the mean of each gene across all samples, resulting in a scale-free dataset. For *A. thaliana*, we collected microarray data from AtGenExpress and processed them as described above. Gene lists were compiled from literature searches and BLAST results using the *A. thaliana* or *P. sativum* genes, and are given in SI Appendix, Tables S1 and S2. Co-expression was visualized with the R package *corrplot*, with the order of genes within each set (proteasome and chloroplast translocon) determined by hierarchical clustering using a combination of "hclust" and "FPC" methods in *corrplot*. The distribution of Pearson correlation coefficient (PCC) values for each gene set was plotted in R using the *density* function. To identify genes that are co-expressed with *C. reinhardtii TIC20*, we calculated the mutual ranks (MR) associated with all gene pairs (*93, 94*) and then converted MR values into network edge weights (an edge being the distance between two genes (or nodes)). For the highest stringency, we opted for the formula with the fastest rate of decay: edge = $e^{-(MR-1)/5}$, and deemed a gene to be co-expressed with *TIC20* only if its network edge weight with *TIC20* was greater than 0.01.

Construction of plasmids

Construction of pRAM73.19

A chloroplast integration plasmid carrying the *psbD* 5'UTR fused to the *tic214 (orf1995)* coding sequence was generated in two sub-cloning steps, as described below. First, 210 bp of the *psbD* promoter and 5'UTR and about 2.4 kbp of the *tic214* coding sequence were amplified from chloroplast genomic DNA using primer pair SR212/SR247 and SRSR246/SR231, respectively. These two PCR products were gel-purified, mixed in an equimolar amount, and used as a template for an overlap extension PCR by SR212/SR231. The resulting PCR product was gel-purified, digested by ClaI and EcoRI, and cloned in the chloroplast integration vector pUCatpXaadA digested with the same restriction enzymes. The resulting plasmid was verified by digestion analysis and named pRAM72. Next, about 2.7 kbp of the region upstream of the *tic214* 5'UTR was amplified from chloroplast genomic DNA using primer pair SR228/SR229. This PCR product was gel-purified, digested by SacI and XbaI, and cloned into pRAM72 digested with the same restriction enzymes. The resulting plasmid was verified by digestion analysis and DNA sequencing and named pRAM73.19. The sequence of the primers used during this cloning are reported below:

SR212 5’-ccatcgatTGTGATGACTATGCACAAAG-3’

SR247 5’-TTTATCATCGTCATCTTTATAATCGAACATtgcgtgtatctccaaaataaaa-3’

SR246 5’-atgttcgattataaagatgacgatgataaaATAACATTTACTTTTATGTCAC-3’

SR231 5'-gGAATTCTCTCCATCTGCTCC-3’

SR228 5’-ggagctcAAGCATTAAATTAAGTTAACTTCAC-3’

SR229 5’-gctcTAGAACCAGCGGCGTTCTTAT-3’

Construction of pED3 (to produce recombinant proteins used to raise the polyclonal antibody against Tic214)

A DNA fragment of *tic214* was amplified from genomic DNA using the primer pair ED5/ED6. This PCR product was gel-purified, digested by NcoI and XhoI, and cloned in the bacterial expression vector pET28a digested with the same restriction enzymes.

The resulting plasmid was verified by digestion analysis and DNA sequencing and named pED3. The sequence of the primers used during this cloning are reported below:
ED5 5'- catgccatggTAAATGTAGCTAAACAAATATTA-3'
ED6 5'- ccgctcgagTGTTTTTCTCCAACGTAAAGT-3'

Construction of the Y14 and NY6 strains

To generate the Y14 strain, the A31 strain (*70*) was transformed with the chloroplast integration plasmid pRAM73.19, where the *aadA* cassette (used as a selective marker) is located just upstream of the *psbD* 5'UTR fused to the *tic214* gene. To generate the NY6 strain, a WT strain was transformed with a chloroplast integration plasmid named Orf1995:HA (NdeI) (gift of E. Boudreau with the HA-11 epitope inserted in the 5' coding sequence of the *tic214* gene. In this vector, *tic214* is under the control of its endogenous 5' UTR, and the *aadA* cassette is adjacent to it. Chloroplast transformation was performed as described (*70*).

Chloroplast isolation

The Chlamydomonas cell wall-deficient strains CC-400 (*cw-15* mt^+) (a kind gift from H. Fukuzawa (Kyoto University), CC-4533 and CS1_FC1D12 (CC-4533 transformed with a *TIC20-YFP-FLAG*$_{3x}$ nuclear transgene – both available at the Chlamydomonas Center) were grown until mid-log phase in TAP medium with shaking at 100 rpm at 25˚C in constant white light (54 µmol $m^{-2}s^{-1}$, provided by fluorescent bulbs). Intact chloroplasts were isolated as described (*95*) with slight modifications as follows: cells were harvested at 3,000 *g* for 4 min at 4˚C and washed with 50 mM Hepes-KOH, pH 7.8. After centrifugation at 3,000 *g* for 5 min at 4˚C, the cells were suspended in isolation buffer [50 mM Hepes-KOH, pH 7.8, 0.3 M sorbitol, 2 mM EDTA, 1 mM $MgCl_2$, 0.1% (w/v) BSA, 0.5% (w/v) sodium ascorbate]. Just before cell breakage, cell suspensions were diluted to 0.5-3 mg chlorophyll / ml with isolation buffer and transferred to a 10 ml-Leuer-lock-syringe. The cells were broken by two passages through a 27-gauge needle at a flow rate of 0.1 ml / s. The suspensions were overlaid onto 45% / 80% Percoll step gradients [45% (v/v) or 80%(v/v) of Percoll, 50 mM Hepes-KOH, pH 6.8, 0.33 M sorbitol, 1 mM $Na_4P_2O_7$, 2 mM EDTA, 1 mM $MgCl_2$, 1 mM $MnCl_2$,

0.3% (w/v) sodium ascorbate] and centrifuged in a swinging-bucket rotor at 4,200 *g* for 15 min at 4˚C. Intact chloroplasts were collected from the 45% - 80% interface, diluted with 5 volumes of HS buffer (50 mM Hepes-KOH, pH 7.8, 0.3 M sorbitol) followed by centrifugation at 1,000 *g* for 3 min at 4˚C, and resuspended in HS buffer. After measuring chlorophyll concentration, chloroplasts were centrifuged at 1,600 *g* for 2 min at 4˚C and stored either on ice or at −80˚C.

Preparation of urea-denatured pre-proteins

To express model pre-proteins in *E. coli*, cDNAs encoding pre-RbcS2, and pre-Fdx1 were obtained by RT-PCR from Chlamydomonas mRNA with the following primers: preRBCS2, CrRBCS2_F1_SpeI (5'-cctactagtGTCATTGCCAAGTCCTCCGTC-3') and CrRBCS2_B1_BglII (5'-ccaagatctCACGGAGCGCTTGTTGGCGGG-3'); preCrFDX1, YACrFd1_F (SpeI) (5'-cttactagtATGGCCATGGCTATGCGCTCC-3') and YACrFd1_R (Bgl II) (5'-cttagatctGTACAGGGCCTCCTCCTGGTG-3'). The cDNAs were cloned into pET24a-FLAG$_{3x}$-TEV-Protein A-HIS$_{6x}$ (*44*) to generate pET24-preCrRBCS2 and pET24-preCrFDX1. Model pre-proteins were expressed in *E. coli* BL21 (DE3) Star (Thermo Fisher Scientific) and purified on His•Bind resin (Novagen) in the presence of 8 M urea according to manufacturer's instructions. The concentrations of pre-proteins were adjusted to 10-20 µM with 8 M urea buffer (8 M urea, 250 mM NaCl, 50 mM Tris-HCl, pH 7.5) and stored at −80˚C until use.

***In vitro* protein import experiments**

In vitro import experiments with isolated intact chloroplasts prepared from Chlamydomonas strain CC-400 and purified pre-proteins were performed as described for *A. thaliana* (*44*) with the following minor modifications. Briefly, pre-proteins pre-RbcS2 and pre-Fdx1 with a C-terminal FLAG$_{3x}$-TEV-Protein A-HIS$_{6x}$ tag were microfuged for 10 - 20 min at 25˚C to remove insoluble materials and denatured again with an equal volume of 8 M urea dilution buffer (8 M urea, 20 mM DTT, 10 mM Hepes-KOH, pH 7.8) immediately before use. Intact chloroplasts (1 - 2 mg chlorophyll) were incubated with denatured pre-proteins (100 - 200 nM) in 3 - 4 ml of HS buffer containing 0, 0.3, or 3 mM Mg-ATP, 5 mM $MgCl_2$, 5 mM DTT) for 15 min at 25˚C in the dark. After

centrifugation at 1,600 *g* for 2 min at 4˚C, chloroplasts were washed twice with HS buffer. Chloroplasts were resuspended with HS buffer with or without (for thermolysin treatment) 0.1 % protease inhibitor cocktail (for plant cells, Sigma, P-9959) and transferred to a new tube. Thermolysin treatment was carried out as previously described (*44*). For purification of translocation intermediates, chloroplasts were pelleted by centrifugation and snap-frozen in liquid nitrogen and stored at −80˚C until use. To obtain soluble fractions containing stromal proteins, chloroplasts suspended in HS buffer containing 0.1% protease inhibitor cocktail were subjected to two freeze-thaw cycles, and the supernatant fraction was obtained after centrifugation at 21,500 *g* for 5 min at 4˚C.

Purification of translocation intermediates

Translocation intermediates after *in vitro* import experiments of model pre-proteins were purified as described for *A. thaliana* (*44*) with slight modifications. Stored chloroplasts were suspended in solubilization buffer (1% water-soluble digitonin, 50 mM Tris-HCl, pH 7.5, 10% [w/v] glycerol, 250 mM NaCl, 5 mM EDTA, 5 mM DTT, 0.5% protease inhibitor cocktail) to a final concentration of 2 mg chlorophyll / mL for 20 min with gentle rotation at 4˚C. To remove insoluble materials, the chloroplast suspension was centrifuged at 21,500 *g* for 2 min at 4˚C, and the supernatant was again ultracentrifuged with a Hitachi S100 AT5 angle rotor at 100,000 *g* for 5 min 4˚C. The resulting supernatant (~1 ml) was incubated with 20 µl of dimethyl pimelimidate (DMP) cross-linked IgG Sepharose 6 Fast Flow (GE healthcare) resin for 2 h with gentle rotation at 4˚C. After washing 4 times with 0.7 ml of 0.2% digitonin-containing TGS buffer (50 mM Tris-HCl, pH 7.5, 10% [w/v] glycerol, 250 mM NaCl, 1 mM DTT), resins were further washed with the same buffer for 5 min with rotation at 4˚C to remove non-specific proteins. The resins were transferred to a siliconized 0.5 ml-tube, and washed twice with 0.5 ml of 0.2% digitonin-containing TGS buffer. Bound translocation intermediates were eluted by cleavage with TEV protease in 100-120 µl of 0.2% digitonin containing TGS buffer for 1 h at 25 ˚C. To capture His-tagged TEV protease, 12 µl of complete His-Tag Purification Resin (Roche) was added and incubated for 15 min at 25˚C. After centrifugation at 8,700 *g* for 1 min at 4˚C, the supernatant was applied on a Micro Bio-

spin column (Bio-Rad) to remove remaining resins, and the resulting flow-through was collected. For SDS-PAGE, the eluates were immediately denatured with sample buffer containing 16.7 mM Tris, pH 6.8, 50 mM (2-carboxyethyl) phosphine hydrochloride (TCEP-HCl) (Sigma, 66547) and 0.1% protease inhibitor cocktail at 37˚C for 30 min. For mass-spec analysis, the eluates were stored on ice until use.

Purification of the Chlamydomonas TicToc supercomplex containing $FLAG_{3x}$-tagged Tic20

Chloroplasts (2-3 mg chlorophylls) isolated from CS1_FC1D12 (a CC-4533 strain transformed with a *TIC20-YFP-$FLAG_{3x}$* nuclear transgene) (were solubilized with digitonin as described for the purification of translocation intermediates. Solubilized proteins were incubated with 15-20 µl of Anti-FLAG M2 Affinity Gel (Sigma) for 2 h with gentle rotation at 4˚C. After similar extensive washing as described above, bound complexes were eluted with 100-120 µl of $FLAG_{3x}$ peptide (100 µg / mL)(Sigma) in 0.2% digitonin containing TGS buffer for 40 min at 4˚C.

Production of Antisera

For expression of the Chlamydomonas Tic56 protein fragment in *E. coli*, the Cre17.g727100 coding sequence corresponding to amino acid residues 114-144 of Chlamydomonas Tic56 was synthesized; 5'-GGTGAACTGCGTCCGGTTCCGCGTAAAATTGTTCTGAGCCCGTATCAGTATGAGATGATTAACTATCAGCGTATGCTGATGCGCAAAAACATTTGGTATTATCGCGATCGTATGAATGTTCCGCGTGGTCCGTGTCCGCTGCATGTTGTTAAAGAAGCATGGGTTAGCGGTATTGTGGATGAAAATACCCTGTTTTGGGGTCATGGTCTGTATGATTGGCTGCCTGCAAAAAACATTAAACTGCTGCTGCCGATGGTTCGTACACCGGAAGTTCGTTTTGCAACCTGGATTAAACGTACCTTTAGCCTGAAACCGAGCCTGAATCGTATTCGTGAACAGCGTAAAGAACATCGTGATCCGCAAGAAGCAAGCCTGCAGGTTGAACTGATGCGT-3'. The synthetic DNA fragment was cloned into the expression vector pGEM-EX1 (Promega) with a C-terminal HIS_{6x}-tag. Polyclonal antiserum against Chlamydomonas Tic56 was produced by immunization of the purified Chlamydomonas Tic56 fragment as an antigen into a guinea pig. To produce the polyclonal antiserum

against Chlamydomonas Tic214, a rabbit was immunized with a recombinant protein fragment corresponding to amino acid residue 628-737 of Chlamydomonas Tic214. This antigen was purified under denaturing conditions starting from BL21 *E.coli* cells transformed with pED3 (for detail, see construction of plasmids). A polyclonal antiserum against Chlamydomonas Tic20 was generated in collaboration with Yenzym, South San Francisco, upon rabbit immunization with the following peptide antigen: CRAEDAEKQDWKFGRNEG.

Protein extraction and immunoblot analysis

Unless stated otherwise, total protein extraction and immunoblot analysis were performed as previously described (*70*). When a TCA protein extraction protocol was employed, the cell pellet was resuspended in 10% TCA in acetone plus 0.07% β-ME. To allow protein precipitation, the lysate was incubated at -20°C for at least 45 min and then subjected to centrifugation at 20,000g at 4°C for 15 min. The pellet was washed with cold acetone containing 0.07% β-ME at least twice. Finally, the pellet was dried with a speed vac and resuspended in a denaturing protein buffer containing 50 mM Tris-HCl pH 6.8, 300 mM NaCl, 2% SDS, and 10 mM EDTA. Prior to immunoblot analysis, the protein content of each sample was measured by BCA assay to ensure equal loading. Transfer to PVDF membranes was carried out with (for Tic214 and others) or without (for Tic56) 0.01% SDS in transfer buffer at 60 V for 2 h or 20 V overnight on ice. Proteins were detected by the ECL Prime Western Blotting System (GE healthcare) or Clarity ECL Western Substrate (Bio-Rad) and exposed to X-ray films (Super RX, Fuji film).

LC-MS/MS analysis of translocation intermediates

After alkylation with iodoacetamide, purified proteins were digested with trypsin in solution. LC-MS/MS analysis was performed by UltiMate 3000 Nano LC systems coupled to Q-Exactive hybrid quadrupole-Orbitrap mass spectrometer (Thermo Fisher Scientific). Peptides and proteins were identified by Mascot v2.3 (Matrix Science, London) searched against the Uniprot Chlamydomonas dataset and the *Creinhardtii*_281_v5.5.protein datasets.

LC-MS/MS analysis of total protein extracts upon Tic214 depletion and proteasome inhibition

Cell pellets preparation: at the beginning of the experiment, 20-ml aliquots of cell culture in the late exponential phase (at a cell density of about 7*10 ^{6} cells / ml) were inoculated and diluted ten times either in regular TAP or TAP freshly supplied with 200 µM Thiamine and 20 µg / ml B12. Thereafter, to keep cell growth in the exponential phase, all cultures were diluted every 24 h to a final cell concentration of about 7*10^{5} cells/ml. At each harvesting time point (2, 4, and 6 days), about 4*10^{8} cells were pelleted at 1000 g for 5 min at RT. After being resuspended in 25 ml of the same type of growth medium (i.e., / + Vit), they were incubated for 3 h in the presence of 30 µM MG132 (Sigma Aldrich #M7449). Then, cells were pelleted again, frozen in liquid nitrogen, and stored at -80°C until use. *Cell pellets processing*: the weight of each frozen cell pellet was measured and resuspended in 5 volumes of lysis buffer containing 100 mM Tris-HCl pH8, 600 mM NaCl, 4% SDS, 20 mM EDTA and freshly supplemented with MS-SAFE Protease and Phosphatase Inhibitor Cocktail (Sigma Aldrich # MSSAFE) (e.g., 100 mg frozen pellet = 500 µl lysis buffer). Cells were disrupted by constant agitation in this buffer for 30 min at 4°C. Then, the protein mixture was further denatured for 30 min at RT and centrifuged at 21000 g for 30 min at 4°C to remove cellular debris. The supernatant (i.e., total protein) was transferred in a clean Eppendorf, and a 5-µl aliquot of this clear lysate was used to determine protein concentration by BCA assay (REF. Perlaza et al. 2019). *Sample preparation for Mass-spec analysis*: for each time point, 60 µg of total protein extracts were mixed with Laemmli sample buffer (Biorad #1610747), freshly supplemented with 2-mercaptoethanol (Biorad #1610710), heated for 30 min at 37°C and loaded into a polyacrylamide gel (any kD™ precast protein gel, Biorad #4569034). To avoid cross-contamination, one empty well was left between the different protein samples. Proteins were allowed to electrophorese into the gel for 15 min at 100 V, visualized by Colloidal Coomassie staining (REF. https://www.ncbi.nlm.nih.gov/pmc/articles/PMC3149902/), excised as a single gel band of 0.5 X 1.5 cm, transferred in a clean Eppendorf tube a

1% acetic acid solution, and sent out to the Stanford University Mass Spec Core. *Mass spec analysis*: the identification of peptides and proteins by tandem mass spectrometry was carried out by the Stanford University Mass Spec Core using the Byonic software package. Output data were organized in two different types of Excel spreadsheets, one for proteins, and one for peptide-spectrum matches (PSMs) and were summarized in a heatmap (*SI Appendix*, Table S10). *Data mining*: Only proteins for which at least 10 MS-peptides could be identified in one of the six conditions were taken into consideration for further analysis. Their localization was predicted using the Predalgo software (*65*). In 80% of the cases (345/427), the chloroplast localization was confirmed by another prediction software, ChloroP (*96*). Only proteins for which sequences derived from their predicted cTP could be detected upon Tic214 were annotated as potential TIC clients. This information is available in *SI Appendix*, Table S11. The PhytoMine interface (https://phytozome.jgi.doe.gov/phytomine) was used to identify potential *A. thaliana* orthologs of these proteins listed in *SI Appendix*, Table S12. To assess whether Tic214 knockdown affects chloroplast stress-responsive proteins encoded by nuclear genes and *MARS1*-dependent genes, we added +1 to all spectral counts, and determined the protein fold-change for each timepoint as $\log_2$ (spectral counts Tic214 OFF / spectral counts Tic214 ON). A protein was considered affected by Tic214 knockdown when its fold change was = or > 2 at least in one timepoint (768 proteins). This information is available in *SI Appendix*, Table S13. Lists of chloroplast stress-responsive genes and *MARS1*-dependent genes were extracted from (*75*). All calculations were done in R (R project v3.5.1) (www.R-project.org) using a combination of the packages stringr (https://CRAN.R-project.org/package=stringr.), dplyr (https://CRAN.R-project.org/package=dplyr.), gplots (. https://CRAN.R-project.org/package=gplots.) and custom scripts.

Miscellaneous

Isolation of RNA and DNA from Chlamydomonas strains and PCRs on genomic DNA to test chloroplast genome homoplasmicity were performed as previously described (*70*). RT-PCRs were performed as previously described (*44*). Mass-spec compatible silver staining was carried out as previously described (*97*). 2D Blue native/SDS-PAGE was

performed as previously described (*98*). Electron microscopy imaging was carried out as previously described (*71*). Co-immunoprecipitation studies shown in Table 1 and *SI Appendix*, Fig. S3 and Tables S6 and S7 were performed as previously described (*61*).

Authors Contributions

S.R., J.D.R, M.N., and P.W. conceived and planned experiments; S.R., Y.A., K.T., and M.C. carried out experiments; L.C.M.M., M.C.J., M.R., and E.D. help to generate critical reagents; S.R., Y.A., P.S., D.S., M.B., K.T., L.M., M.H., M.N., J.D.R., and P.W. analyzed data; S.R. and P.W. wrote the manuscript with inputs from all authors. All authors read and approved the manuscript.

Acknowledgments

We thank Christopher M. Adams and Ryan Leib from the Stanford University Mass Spectrometry Platform for carrying out mass-spectrometry analysis, Lorenzo Costantino, Elif Karagoz, and Jan Schuller for useful feedback on the manuscript. This project was supported by an EMBO long term-fellowship (ALTF 563-2013) and a Swiss National Science Foundation Advanced PostDoc Mobility Fellowship (P2GEP3_148531) awarded to SR, a Belgian-American Educational Foundation fellowship to M.B., a Humboldt Research Fellowship awarded to L.M., a Deutsche Forschungsgemeinschaft grant (HI 739/9.1 and HI 739/9.2) awarded to M.H., two grants from Ministry of Education Culture, Sports, Science and Technology (17H05668 and 17H05725) awarded to MN, a cooperative agreement of the US Department of Energy Office of Science, Office of Biological and Environmental Research program (DE-FC02-02ER63421) awarded to Sabeeha Merchant and Todd Yeates (UCLA), and a grant from the Swiss National Foundation (31003A_133089/1) awarded to JDR. PW is an Investigator of the Howard Hughes Medical Institute (HHMI826735-0012) and is supported by the National Institute of Health (R01GM032384).

References

1. L. Margulis, Symbiotic theory of the origin of eukaryotic organelles; criteria for proof. *Symp Soc Exp Biol*, 21-38 (1975).
2. G. Van den Broeck *et al.*, Targeting of a foreign protein to chloroplasts by fusion to the transit peptide from the small subunit of ribulose 1,5-bisphosphate carboxylase. *Nature* **313**, 358-363 (1985).
3. S. Smeekens, C. Bauerle, J. Hageman, K. Keegstra, P. Weisbeek, The role of the transit peptide in the routing of precursors toward different chloroplast compartments. *Cell* **46**, 365-375 (1986).
4. B. Dobberstein, G. Blobel, N. H. Chua, In vitro synthesis and processing of a putative precursor for the small subunit of ribulose-1,5-bisphosphate carboxylase of Chlamydomonas reinhardtii. *Proc Natl Acad Sci U S A* **74**, 1082-1085 (1977).
5. N. H. Chua, G. W. Schmidt, Post-translational transport into intact chloroplasts of a precursor to the small subunit of ribulose-1,5-bisphosphate carboxylase. *Proc Natl Acad Sci U S A* **75**, 6110-6114 (1978).
6. P. M. Kirwin, P. D. Elderfield, C. Robinson, Transport of proteins into chloroplasts. Partial purification of a thylakoidal processing peptidase involved in plastocyanin biogenesis. *J Biol Chem* **262**, 16386-16390 (1987).
7. D. Pain, Y. S. Kanwar, G. Blobel, Identification of a receptor for protein import into chloroplasts and its localization to envelope contact zones. *Nature* **331**, 232-237 (1988).
8. D. J. Schnell, F. Kessler, G. Blobel, Isolation of components of the chloroplast protein import machinery. *Science* **266**, 1007-1012 (1994).
9. M. Akita, E. Nielsen, K. Keegstra, Identification of protein transport complexes in the chloroplastic envelope membranes via chemical cross-linking. *J Cell Biol* **136**, 983-994 (1997).
10. F. Kessler, G. Blobel, H. A. Patel, D. J. Schnell, Identification of two GTP-binding proteins in the chloroplast protein import machinery. *Science* **266**, 1035-1039 (1994).
11. J. Bauer *et al.*, The major protein import receptor of plastids is essential for chloroplast biogenesis. *Nature* **403**, 203-207 (2000).
12. D. J. Schnell, G. Blobel, Identification of intermediates in the pathway of protein import into chloroplasts and their localization to envelope contact sites. *J Cell Biol* **120**, 103-115 (1993).
13. P. Chotewutmontri, K. Holbrook, B. D. Bruce, Plastid Protein Targeting: Preprotein Recognition and Translocation. *Int Rev Cell Mol Biol* **330**, 227-294 (2017).
14. Y. D. Paila, L. G. L. Richardson, D. J. Schnell, New insights into the mechanism of chloroplast protein import and its integration with protein quality control, organelle biogenesis and development. *J Mol Biol* **427**, 1038-1060 (2015).
15. L. X. Shi, S. M. Theg, The chloroplast protein import system: from algae to trees. *Biochim Biophys Acta* **1833**, 314-331 (2013).
16. S. M. Thomson, P. Pulido, R. P. Jarvis, Protein import into chloroplasts and its regulation by the ubiquitin-proteasome system. *Biochem Soc Trans* **48**, 71-82 (2020).
17. F. Kessler, D. Schnell, Chloroplast biogenesis: diversity and regulation of the protein import apparatus. *Curr Opin Cell Biol* **21**, 494-500 (2009).
18. H. M. Li, C. C. Chiu, Protein transport into chloroplasts. *Annu Rev Plant Biol* **61**, 157-180 (2010).
19. L. G. L. Richardson, D. J. Schnell, Origins, function, and regulation of the TOC-TIC general protein import machinery of plastids. *J Exp Bot* **71**, 1226-1238 (2020).
20. D. J. Schnell *et al.*, A consensus nomenclature for the protein-import components of the chloroplast envelope. *Trends Cell Biol* **7**, 303-304 (1997).

21. K. Cline, J. Andrews, B. Mersey, E. H. Newcomb, K. Keegstra, Separation and characterization of inner and outer envelope membranes of pea chloroplasts. *Proc Natl Acad Sci U S A* **78**, 3595-3599 (1981).
22. S. E. Perry, K. Keegstra, Envelope membrane proteins that interact with chloroplastic precursor proteins. *Plant Cell* **6**, 93-105 (1994).
23. A. Kouranov, D. J. Schnell, Analysis of the interactions of preproteins with the import machinery over the course of protein import into chloroplasts. *J Cell Biol* **139**, 1677-1685 (1997).
24. A. Caliebe *et al.*, The chloroplastic protein import machinery contains a Rieske-type iron-sulfur cluster and a mononuclear iron-binding protein. *EMBO J* **16**, 7342-7350 (1997).
25. A. Kouranov, X. Chen, B. Fuks, D. J. Schnell, Tic20 and Tic22 are new components of the protein import apparatus at the chloroplast inner envelope membrane. *J Cell Biol* **143**, 991-1002 (1998).
26. T. Stahl, C. Glockmann, J. Soll, L. Heins, Tic40, a new "old" subunit of the chloroplast protein import translocon. *J Biol Chem* **274**, 37467-37472 (1999).
27. M. Kuchler, S. Decker, F. Hormann, J. Soll, L. Heins, Protein import into chloroplasts involves redox-regulated proteins. *EMBO J* **21**, 6136-6145 (2002).
28. F. Hormann *et al.*, Tic32, an essential component in chloroplast biogenesis. *J Biol Chem* **279**, 34756-34762 (2004).
29. X. Chen, M. D. Smith, L. Fitzpatrick, D. J. Schnell, In vivo analysis of the role of atTic20 in protein import into chloroplasts. *Plant Cell* **14**, 641-654 (2002).
30. T. Inaba *et al.*, Arabidopsis tic110 is essential for the assembly and function of the protein import machinery of plastids. *Plant Cell* **17**, 1482-1496 (2005).
31. P. Jarvis *et al.*, An Arabidopsis mutant defective in the plastid general protein import apparatus. *Science* **282**, 100-103 (1998).
32. D. Constan, R. Patel, K. Keegstra, P. Jarvis, An outer envelope membrane component of the plastid protein import apparatus plays an essential role in Arabidopsis. *Plant J* **38**, 93-106 (2004).
33. Y. S. Teng *et al.*, Tic21 is an essential translocon component for protein translocation across the chloroplast inner envelope membrane. *Plant Cell* **18**, 2247-2257 (2006).
34. P. Boij, R. Patel, C. Garcia, P. Jarvis, H. Aronsson, In vivo studies on the roles of Tic55-related proteins in chloroplast protein import in Arabidopsis thaliana. *Mol Plant* **2**, 1397-1409 (2009).
35. Y. Hirabayashi, S. Kikuchi, M. Oishi, M. Nakai, In vivo studies on the roles of two closely related Arabidopsis Tic20 proteins, AtTic20-I and AtTic20-IV. *Plant Cell Physiol* **52**, 469-478 (2011).
36. S. Bischof *et al.*, Plastid proteome assembly without Toc159: photosynthetic protein import and accumulation of N-acetylated plastid precursor proteins. *Plant Cell* **23**, 3911-3928 (2011).
37. M. Sommer *et al.*, Toc33 and Toc64-III cooperate in precursor protein import into the chloroplasts of Arabidopsis thaliana. *Plant Cell Environ* **36**, 970-983 (2013).
38. S. Reumann, J. Davila-Aponte, K. Keegstra, The evolutionary origin of the protein-translocating channel of chloroplastic envelope membranes: identification of a cyanobacterial homolog. *Proc Natl Acad Sci U S A* **96**, 784-789 (1999).
39. C. Andres, B. Agne, F. Kessler, The TOC complex: preprotein gateway to the chloroplast. *Biochim Biophys Acta* **1803**, 715-723 (2010).
40. N. Sveshnikova, R. Grimm, J. Soll, E. Schleiff, Topology studies of the chloroplast protein import channel Toc75. *Biol Chem* **381**, 687-693 (2000).
41. S. C. Hinnah, R. Wagner, N. Sveshnikova, R. Harrer, J. Soll, The chloroplast protein import channel Toc75: pore properties and interaction with transit peptides. *Biophys J* **83**, 899-911 (2002).

42. S. Kikuchi *et al.*, A 1-megadalton translocation complex containing Tic20 and Tic21 mediates chloroplast protein import at the inner envelope membrane. *Plant Cell* **21**, 1781-1797 (2009).
43. E. Kovacs-Bogdan, J. P. Benz, J. Soll, B. Bolter, Tic20 forms a channel independent of Tic110 in chloroplasts. *BMC Plant Biol* **11**, 133 (2011).
44. S. Kikuchi *et al.*, Uncovering the protein translocon at the chloroplast inner envelope membrane. *Science* **339**, 571-574 (2013).
45. J. H. Campbell, T. Hoang, M. Jelokhani-Niaraki, M. D. Smith, Folding and self-association of atTic20 in lipid membranes: implications for understanding protein transport across the inner envelope membrane of chloroplasts. *BMC Biochem* **15**, 29 (2014).
46. L. Heins *et al.*, The preprotein conducting channel at the inner envelope membrane of plastids. *EMBO J* **21**, 2616-2625 (2002).
47. T. Inaba, M. Li, M. Alvarez-Huerta, F. Kessler, D. J. Schnell, atTic110 functions as a scaffold for coordinating the stromal events of protein import into chloroplasts. *J Biol Chem* **278**, 38617-38627 (2003).
48. S. Kovacheva *et al.*, In vivo studies on the roles of Tic110, Tic40 and Hsp93 during chloroplast protein import. *Plant J* **41**, 412-428 (2005).
49. J. Y. Tsai *et al.*, Structural characterizations of the chloroplast translocon protein Tic110. *Plant J* **75**, 847-857 (2013).
50. S. Kikuchi *et al.*, A Ycf2-FtsHi heteromeric AAA-ATPase complex is required for chloroplast protein import. *Plant Cell*, (2018).
51. D. Kohler *et al.*, Characterization of chloroplast protein import without Tic56, a component of the 1-megadalton translocon at the inner envelope membrane of chloroplasts. *Plant Physiol* **167**, 972-990 (2015).
52. B. Bolter, J. Soll, Ycf1/Tic214 Is Not Essential for the Accumulation of Plastid Proteins. *Mol Plant* **10**, 219-221 (2017).
53. J. de Vries, F. L. Sousa, B. Bolter, J. Soll, S. B. Gould, YCF1: A Green TIC? *Plant Cell* **27**, 1827-1833 (2015).
54. M. Nakai, The TIC complex uncovered: The alternative view on the molecular mechanism of protein translocation across the inner envelope membrane of chloroplasts. *Biochim Biophys Acta* **1847**, 957-967 (2015b).
55. M. Nakai, YCF1: A Green TIC: Response to the de Vries et al. Commentary. *Plant Cell* **27**, 1834-1838 (2015a).
56. S. F. Altschul, W. Gish, W. Miller, E. W. Myers, D. J. Lipman, Basic local alignment search tool. *J Mol Biol* **215**, 403-410 (1990).
57. H. Ge, Z. Liu, G. M. Church, M. Vidal, Correlation between transcriptome and interactome mapping data from Saccharomyces cerevisiae. *Nat Genet* **29**, 482-486 (2001).
58. R. Jansen, D. Greenbaum, M. Gerstein, Relating whole-genome expression data with protein-protein interactions. *Genome Res* **12**, 37-46 (2002).
59. N. Simonis, J. van Helden, G. N. Cohen, S. J. Wodak, Transcriptional regulation of protein complexes in yeast. *Genome Biol* **5**, R33 (2004).
60. S. E. Moghadam Marcel Alavi-Khorassani, Analysis of expression patterns of translocon subunits of chloroplasts and mitochondria. *Plant science* **168**, 1533-1539 (2005).
61. L. C. M. Mackinder *et al.*, A Spatial Interactome Reveals the Protein Organization of the Algal CO2-Concentrating Mechanism. *Cell* **171**, 133-147 e114 (2017).
62. E. Boudreau *et al.*, A large open reading frame (orf1995) in the chloroplast DNA of Chlamydomonas reinhardtii encodes an essential protein. *Mol Gen Genet* **253**, 649-653 (1997).

63. L. J. Chen, H. M. Li, Stable megadalton TOC-TIC supercomplexes as major mediators of protein import into chloroplasts. *Plant J* **92**, 178-188 (2017).
64. J. E. Boynton, N. W. Gillham, Chloroplast transformation in Chlamydomonas. *Methods Enzymol* **217**, 510-536 (1993).
65. M. Tardif *et al.*, PredAlgo: a new subcellular localization prediction tool dedicated to green algae. *Mol Biol Evol* **29**, 3625-3639 (2012).
66. X. Li *et al.*, A genome-wide algal mutant library and functional screen identifies genes required for eukaryotic photosynthesis. *Nat Genet* **51**, 627-635 (2019).
67. D. Strenkert *et al.*, Multiomics resolution of molecular events during a day in the life of Chlamydomonas. *Proc Natl Acad Sci U S A* **116**, 2374-2383 (2019).
68. S. D. Gallaher *et al.*, High-throughput sequencing of the chloroplast and mitochondrion of Chlamydomonas reinhardtii to generate improved de novo assemblies, analyze expression patterns and transcript speciation, and evaluate diversity among laboratory strains and wild isolates. *Plant J* **93**, 545-565 (2018).
69. K. Cline, M. Werner-Washburne, J. Andrews, K. Keegstra, Thermolysin is a suitable protease for probing the surface of intact pea chloroplasts. *Plant Physiol* **75**, 675-678 (1984).
70. S. Ramundo, M. Rahire, O. Schaad, J. D. Rochaix, Repression of essential chloroplast genes reveals new signaling pathways and regulatory feedback loops in Chlamydomonas. *Plant Cell* **25**, 167-186 (2013).
71. S. Ramundo *et al.*, Conditional Depletion of the Chlamydomonas Chloroplast ClpP Protease Activates Nuclear Genes Involved in Autophagy and Plastid Protein Quality Control. *Plant Cell* **26**, 2201-2222 (2014).
72. S. Ramundo, J. D. Rochaix, Controlling expression of genes in the unicellular alga Chlamydomonas reinhardtii with a vitamin-repressible riboswitch. *Methods Enzymol* **550**, 267-281 (2015).
73. L. G. Heredia-Martinez, A. Andres-Garrido, E. Martinez-Force, M. E. Perez-Perez, J. L. Crespo, Chloroplast Damage Induced by the Inhibition of Fatty Acid Synthesis Triggers Autophagy in Chlamydomonas. *Plant Physiol* **178**, 1112-1129 (2018).
74. U. W. Goodenough, The effects of inhibitors of RNA and protein synthesis on chloroplast structure and function in wild-type Chlamydomonas reinhardtii. *J Cell Biol* **50**, 35-49 (1971).
75. K. Perlaza *et al.*, The Mars1 kinase confers photoprotection through signaling in the chloroplast unfolded protein response. *Elife* **8**, (2019).
76. S. Ramundo, J. D. Rochaix, Chloroplast unfolded protein response, a new plastid stress signaling pathway? *Plant Signal Behav* **9**, e972874 (2014).
77. E. Llamas, P. Pulido, M. Rodriguez-Concepcion, Interference with plastome gene expression and Clp protease activity in Arabidopsis triggers a chloroplast unfolded protein response to restore protein homeostasis. *PLoS Genet* **13**, e1007022 (2017).
78. J. D. Rochaix, S. Ramundo, Chloroplast signaling and quality control. *Essays Biochem* **62**, 13-20 (2018).
79. V. Dogra, J. Duan, K. P. Lee, C. Kim, Impaired PSII proteostasis triggers a UPR-like response in the var2 mutant of Arabidopsis. *J Exp Bot* **70**, 3075-3088 (2019).
80. S. Lee *et al.*, Heat shock protein cognate 70-4 and an E3 ubiquitin ligase, CHIP, mediate plastid-destined precursor degradation through the ubiquitin-26S proteasome system in Arabidopsis. *Plant Cell* **21**, 3984-4001 (2009).
81. X. Yang, Y. Li, M. Qi, Y. Liu, T. Li, Targeted Control of Chloroplast Quality to Improve Plant Acclimation: From Protein Import to Degradation. *Front Plant Sci* **10**, 958 (2019).
82. B. Kmiec, P. F. Teixeira, E. Glaser, Shredding the signal: targeting peptide degradation in mitochondria and chloroplasts. *Trends Plant Sci* **19**, 771-778 (2014).

83. P. F. Teixeira, E. Glaser, Processing peptidases in mitochondria and chloroplasts. *Biochim Biophys Acta* **1833**, 360-370 (2013).
84. M. Kessel *et al.*, Homology in structural organization between E. coli ClpAP protease and the eukaryotic 26 S proteasome. *J Mol Biol* **250**, 587-594 (1995).
85. B. L. Gutman, K. K. Niyogi, Chlamydomonas and Arabidopsis. A dynamic duo. *Plant Physiol* **135**, 607-610 (2004).
86. J. D. Woodson, J. Chory, Coordination of gene expression between organellar and nuclear genomes. *Nat Rev Genet* **9**, 383-395 (2008).
87. A. Biehl, E. Richly, C. Noutsos, F. Salamini, D. Leister, Analysis of 101 nuclear transcriptomes reveals 23 distinct regulons and their relationship to metabolism, chromosomal gene distribution and co-ordination of nuclear and plastid gene expression. *Gene* **344**, 33-41 (2005).
88. P. Pulido *et al.*, CHLOROPLAST RIBOSOME ASSOCIATED Supports Translation under Stress and Interacts with the Ribosomal 30S Subunit. *Plant Physiol* **177**, 1539-1554 (2018).
89. Y. L. Chen *et al.*, TIC236 links the outer and inner membrane translocons of the chloroplast. *Nature*, (2018).
90. B. Agne, D. Kohler, S. Baginsky, Protein import-independent functions of Tic56, a component of the 1-MDa translocase at the inner chloroplast envelope membrane. *Plant Signal Behav* **12**, e1284726 (2017).
91. D. S. Gorman, R. P. Levine, Cytochrome *f* and plastocyanin: their sequence in the photoelectric transport chain. *Proceedings of the National Academy of Sciences* **54**, 1665-1669 (1966).
92. E. H. Harris, *The Chlamydomonas Source Book : a Comprehensive Guide to Biology and Laboratory Use.*, (Academic Press, Inc., San Diego, CA, 1989).
93. Y. Aoki, Y. Okamura, H. Ohta, K. Kinoshita, T. Obayashi, ALCOdb: Gene Coexpression Database for Microalgae. *Plant Cell Physiol* **57**, e3 (2016).
94. J. H. Wisecaver *et al.*, A Global Coexpression Network Approach for Connecting Genes to Specialized Metabolic Pathways in Plants. *Plant Cell* **29**, 944-959 (2017).
95. C. B. Mason, T. M. Bricker, J. V. Moroney, A rapid method for chloroplast isolation from the green alga Chlamydomonas reinhardtii. *Nat Protoc* **1**, 2227-2230 (2006).
96. O. Emanuelsson, H. Nielsen, G. von Heijne, ChloroP, a neural network-based method for predicting chloroplast transit peptides and their cleavage sites. *Protein Sci* **8**, 978-984 (1999).
97. A. Shevchenko, M. Wilm, O. Vorm, M. Mann, Mass spectrometric sequencing of proteins silver-stained polyacrylamide gels. *Anal Chem* **68**, 850-858 (1996).
98. S. Kikuchi, J. Bedard, M. Nakai, One- and two-dimensional blue native-PAGE and immunodetection of low-abundance chloroplast membrane protein complexes. *Methods Mol Biol* **775**, 3-17 (2011).

List and titles of Main Figures

List and titles of Main Tables

List and titles of Supplementary Figures

Fig. S6. Distribution of Tic214-derived peptides identified by LC-MS/MS analysis of the translocation intermediates.
(Supplemental data for Fig. 4 and Table 2)

Fig. S7. Homoplasmicity of the Y14 strain.
(Supplemental data for Fig. 5 and Fig. 6)

Fig. S8. Chloroplast-stress responsive proteins differentially expressed upon Tic214 depletion.
(Supplemental data for Fig. 6 and Fig. 7)

List and titles of Supplementary Tables

Table S1. Arabidopsis components of the TOC complex and their putative Chlamydomonas orthologs from BLAST analysis.
(Supplemental data for Fig. 1)

Table S2. Proposed Arabidopsis components of the translocon TIC complex and their putative Chlamydomonas orthologs from BLAST analysis.
(Supplemental data for Fig. 1 and Fig. 2)

Table S3. *(Excel file)* List of genes of the components of the proteasome and chloroplast translocons of Chlamydomonas shown in Fig. 1 *A* and *B*, respectively.
(Supplemental data for Fig. 1)

Table S4. *(Excel file)* Statistical table related to data shown in Fig. 1, Fig. 2 and Fig. S1

Table S5. *(Excel file)* List of genes of the components of the proteasome and chloroplast translocons of Arabidopsis shown in Fig. S1 *A* and *B*, respectively.

Table S6. *(Excel file)* LC-MS/MS identification of proteins co-immunoprecipitated with Chlamydomonas Tic20.
(Supplemental data for Fig. 2 and Table1)

Table S7. *(Excel file)* LC-MS/MS identification of proteins co-immunoprecipitated with Chlamydomonas Tic214.
(Supplemental data for Fig. 2 and Table1)

Table S8. Genes co-expressed with Chlamydomonas *TIC20*.
(Supplemental data for Fig. 2)

Table S9. (*Excel file*) LC-MS/MS identification of co-purified proteins with pre-CrRbcS2-$FLAG_{3x}$:Protein A:HIS_{6x} translocation intermediates.
(Supplemental data for Fig. 4 and Table 2)

Table S10. (*Excel file*) LC-MS/MS identification of proteins upon depletion of Ti214 in Chlamydomonas cells.
(Supplemental data for Fig. 7)

Table S11. Chlamydomonas proteins retaining their chloroplast transit peptide upon depletion of CrTi214
(Supplemental data for Fig. 7)

Table S12. Putative Arabidopsis orthologs of Chlamydomonas chloroplast proteins whose import is affected upon depletion of Tic214
(Supplemental data for Fig. 7)

Table S13. (*Excel file*) List of proteins encoded by Chlamydomonas chloroplast stress-responsive and *MARS1*-dependent genes detected by mass spectrometry depletion of Ti214
(Supplemental data for Fig. S8)

Figure 1

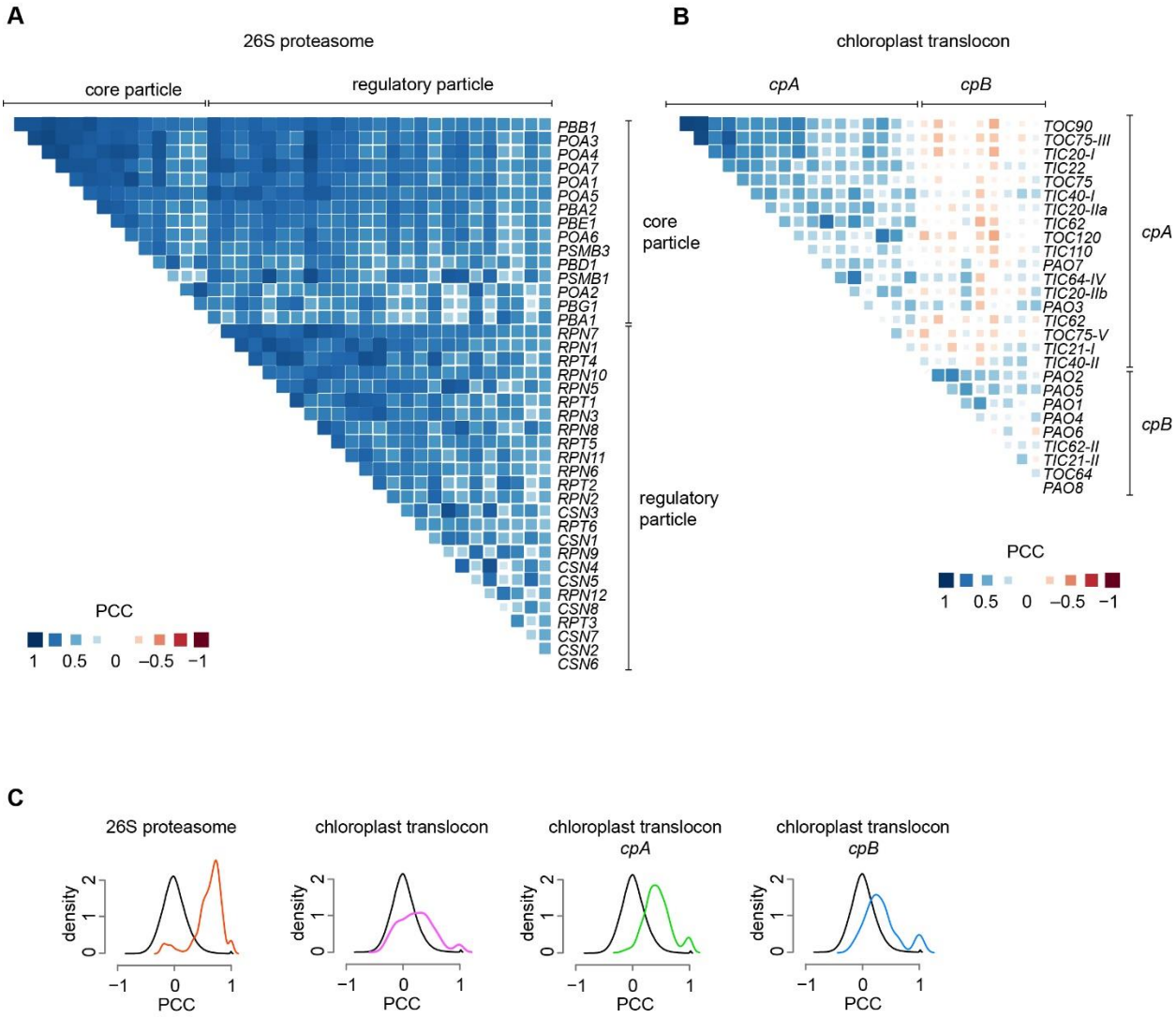

Fig. 1. Co-expression patterns of Chlamydomonas genes encoding components of the plastid translocon.

(*A*) Correlation matrix for Chlamydomonas genes encoding subunits of the 26S proteasome (listed in *SI Appendix*, Table S3).
(*B*) Correlation matrix for Chlamydomonas genes encoding components of the chloroplast translocon identified through BLAST analysis (listed in *SI Appendix*, Table S3).
(*C*) Distribution of Pearson's correlation coefficients (PCCs) for all gene pairs encoding core and regulatory particles of the 26S proteasome (red line), and gene pairs for the chloroplast translocon components, together (magenta line) or as a function of their subgroup, *cpA* (green line) and *cpB* (blue line). PCC distribution for all gene pairs in the genome (black line) is shown to indicate the absence of correlation (i.e. negative control). Statistical significance of all distributions was tested by Kolmogorov-Smirnov test,

comparing each sets of PCC values with a randomly generated normal distribution of equal element number. The results of this analysis are available in *SI Appendix*, Table S4.

Figure 2

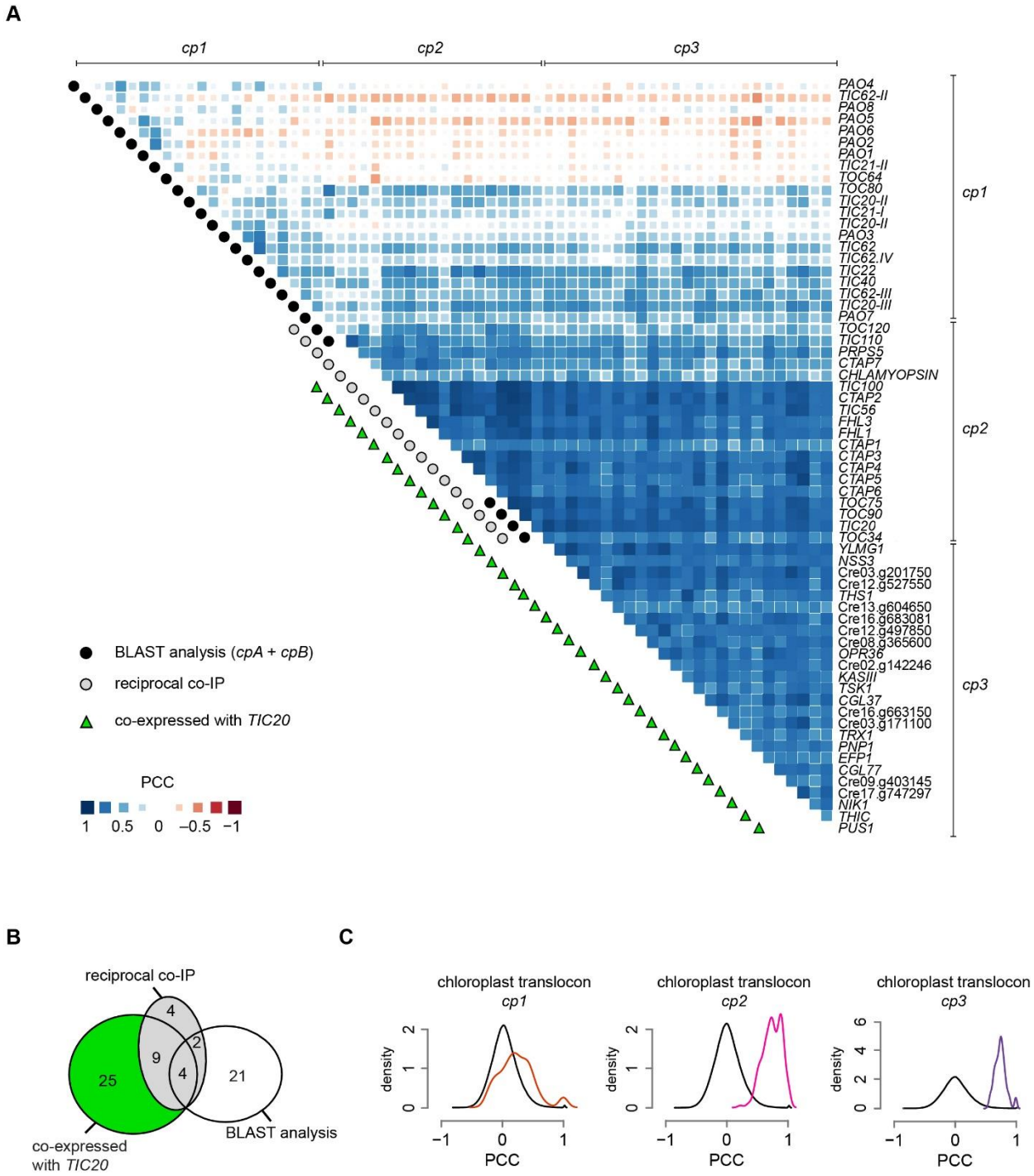

Fig. 2. Co-expression patterns of known and newly identified chloroplast translocon components in Chlamydomonas.

(*A*) Correlation matrix of chloroplast translocon genes from subgroups *cp1* (comprising most of *cpA* and *cpB* genes shown in Fig. 1A), subgroup *cp2* (containing genes identified during both Tic20 and Tic214 pull-downs and listed in Table 1) and subgroup *cp3* (comprising genes only co-expressed with *TIC20* and listed in *SI Appendix*, Table S8).
(*B*) Venn diagram related to gene subgroups shown in panel A.
(*C*) PCC distributions for genes belonging to subgroups *cp1* (red line), *cp2* (magenta line), and *cp3* (purple line) and for all gene pairs in the genome (black line) used as negative control. Statistical significance of all distributions was tested by Kolmogorov-Smirnov test, comparing each sets of PCC values with a randomly generated normal distribution of equal element number. The results of this analysis are available in *SI Appendix*, Table S4.

Figure 3

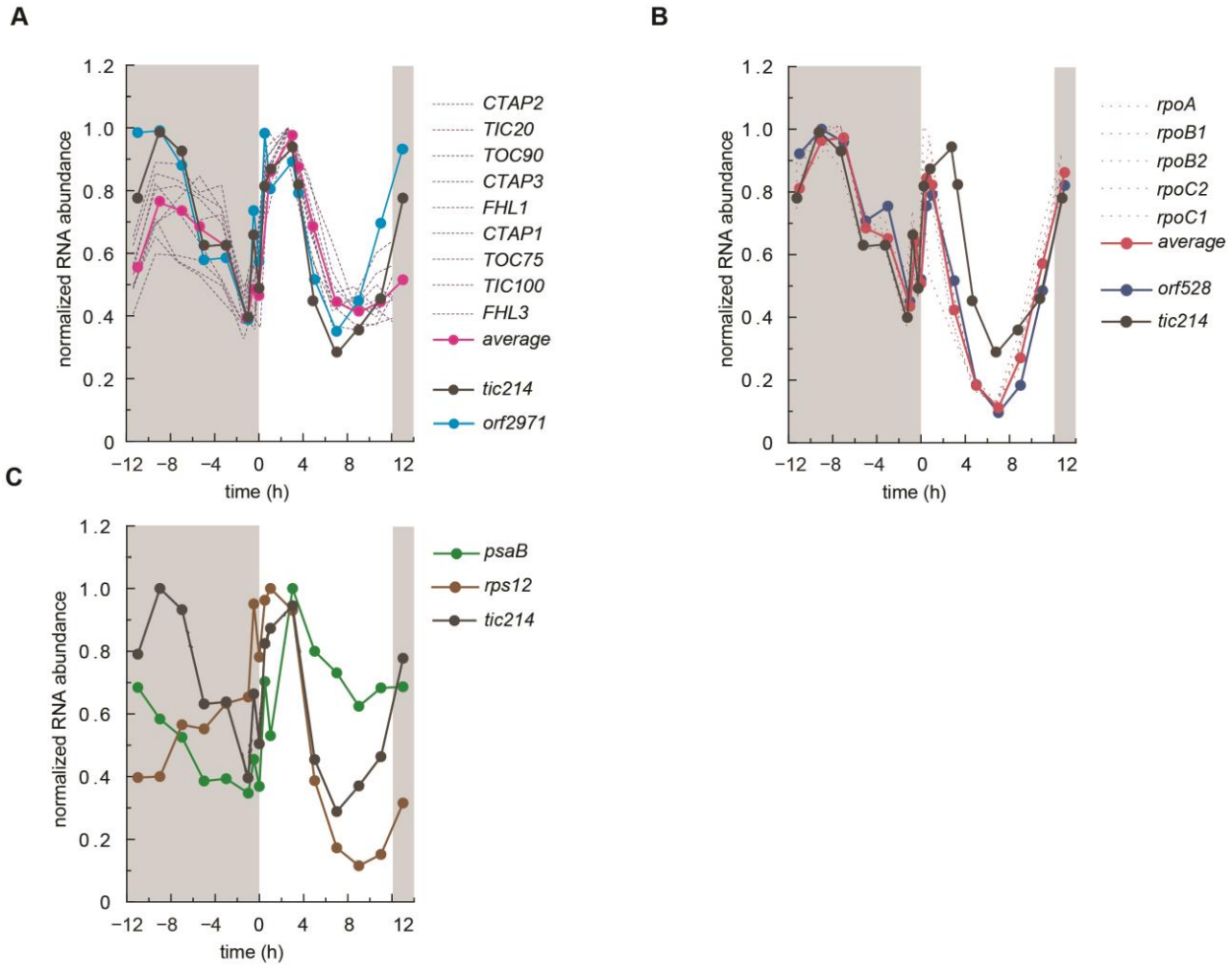

Fig. 3. Co-expression profiles of chloroplast-encoded and nucleus-encoded translocon components over the course of a diurnal cycle in Chlamydomonas.

(*A*) *tic214* (*orf1995*) (black) and *orf2971* (light blue), and co-expressed nucleus-encoded translocon components (blue).
(*B*) *tic214* (black), *orf528* (blue) and co-expressed plastid-encoded RNA polymerase genes (PEP) (dark red).
(*C*) *tic214* (black), *psaB* (green) and *rps12* (brown).

Figure 4

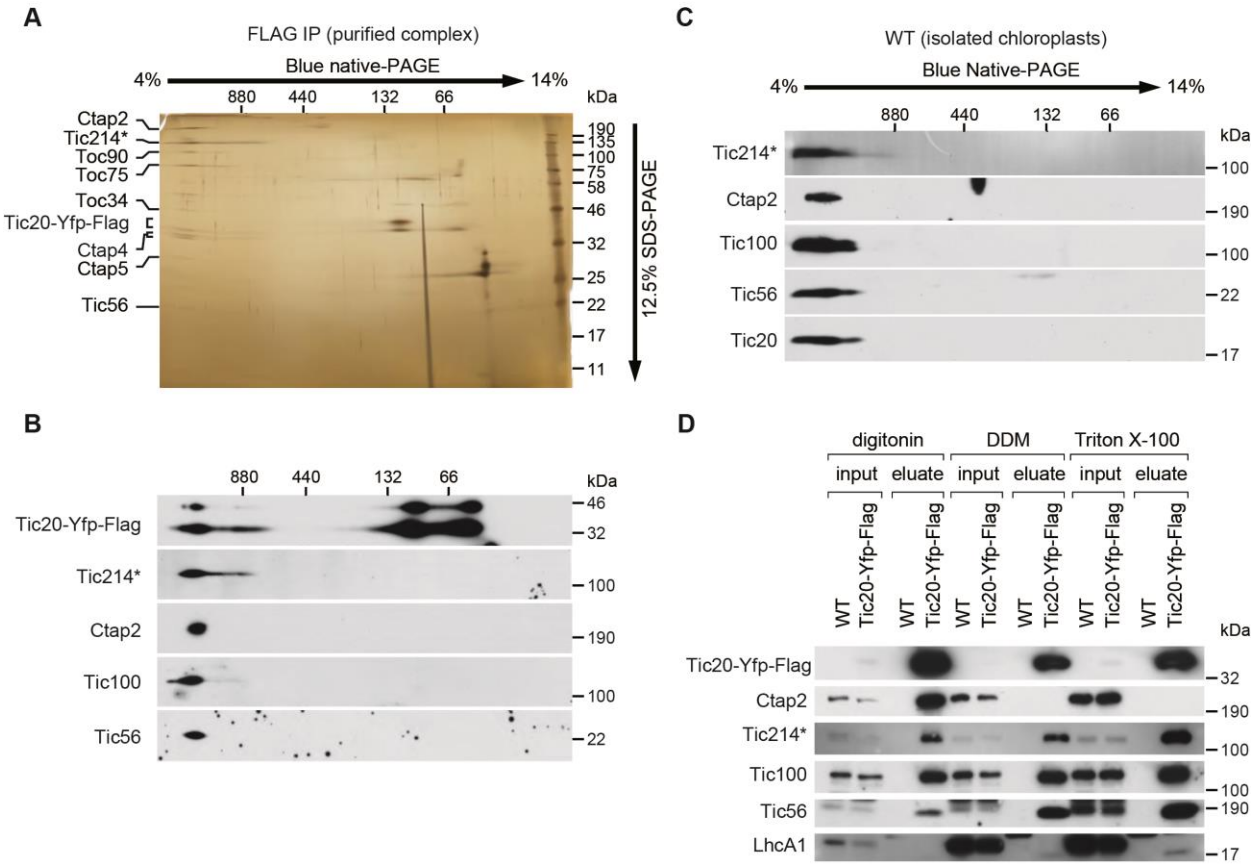

Fig. 4. Tic20 is part of a stable chloroplast translocon supercomplex in Chlamydomonas.

(*A*) 2D blue native/SDS-PAGE separation of the purified Tic20-YFP-FLAG$_{3x}$ fraction (in the presence of digitonin) followed by silver staining. Proteins identified by mass-spec analysis are indicated.

(*B*) Proteins were separated as in panel A and analyzed by immunoblotting with the indicated antibodies.

(*C*) Isolated chloroplasts were solubilized with digitonin and analyzed as in panel A.

(*D*) Purification of the Tic20-YFP-FLAG$_{3x}$ containing supercomplex was carried out after solubilization with digitonin, dodecylmaltoside (DDM), or Triton X-100. The purified fractions (eluate) together with 1% of the input fractions used for the purification (input) were analyzed by SDS-PAGE and immunoblotting with the indicated antibodies. Mock-purified fractions (WT) were also analyzed. Tic214* in panels *A*, *B*, *C,* and *D* denotes the 110 kDa protein band detected by the Tic214 antibody.

Figure 5

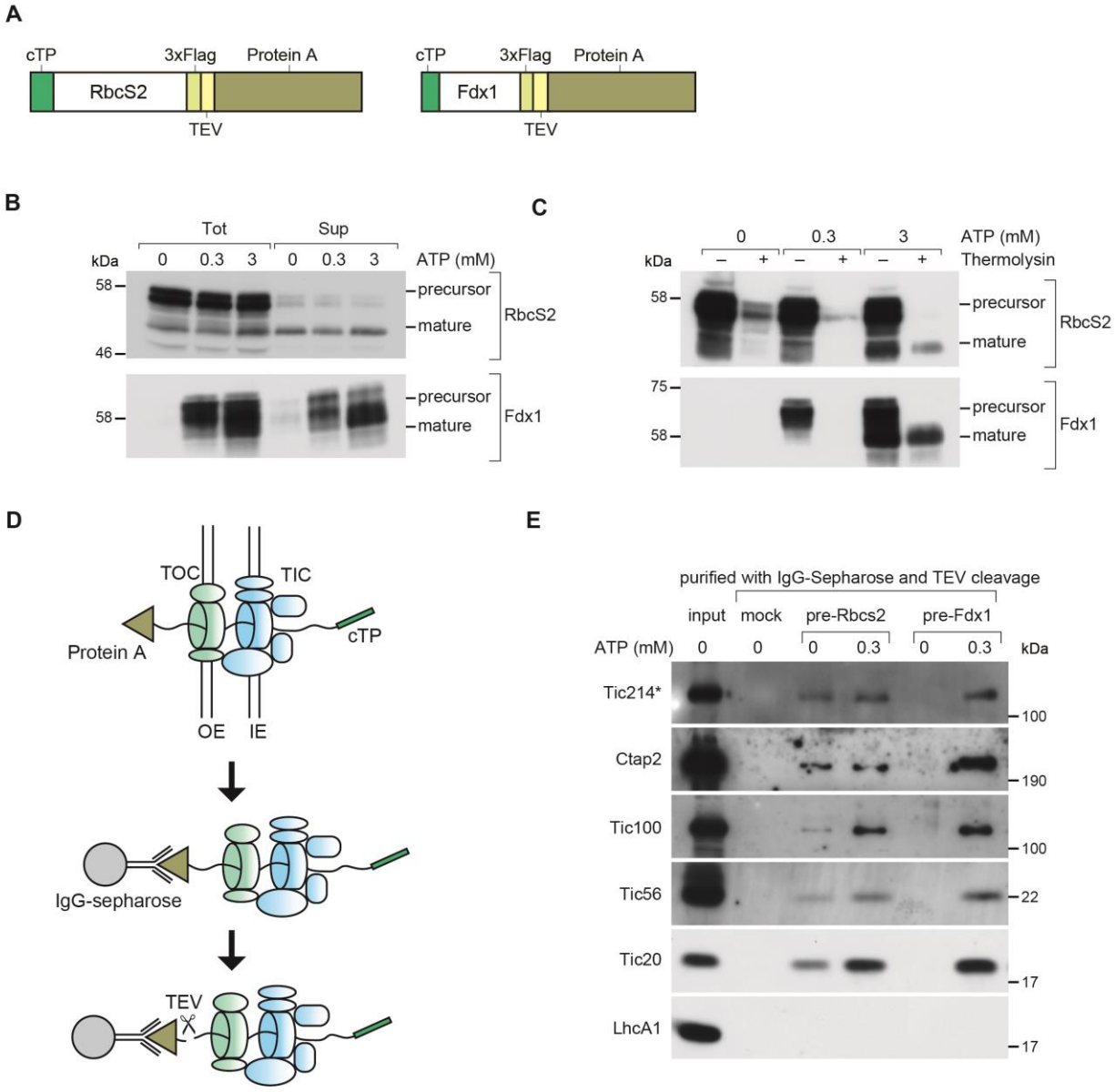

Fig. 5. *In vitro* import assay of chloroplast pre-proteins and purification of translocation intermediates in Chlamydomonas.

(*A*) Schematic representation of the two chloroplast pre-proteins used for *in vitro* import assays and the purification of translocation intermediates.

(*B*) Chloroplast pre-proteins were incubated with intact chloroplasts isolated from Chlamydomonas in the presence of the indicated concentrations of ATP. Chloroplasts were re-isolated, washed, and directly analyzed ("Tot") or fractionated into soluble fraction containing stroma ("Sup").

(*C*) Same assay as in panel B, except that chloroplasts were treated with thermolysin after protein import. In (*B*), a band corresponding to the mature form of RbcS2 is

detected in the absence of ATP and recovered in the Sup fraction. This band does not represent fully translocated protein but is most likely formed or released during the freeze-thaw cycles used for chloroplast lysis. This notion was verified in (*C*) with thermolysin treatment, which shows that there is no fully translocated mature RbcS2 in the absence of ATP. The RbcS2 import experiment was repeated several times with similar band profiles.

(*D*) Outline of the method used to isolate chloroplast intermediate translocation complexes. After import, washed chloroplasts were solubilized with digitonin, and translocation intermediates were purified with IgG-Sepharose and eluted by TEV protease cleavage. Mock purification was carried out without the addition of pre-proteins. IE, OE, inner, outer envelope membrane, respectively.

(*E*) Purified fractions shown in panel D were analyzed by SDS-PAGE and immunoblotting with the indicated antibodies. Tic214* denotes the 110 kDa protein band detected by the Tic214 antibody.

Figure 6

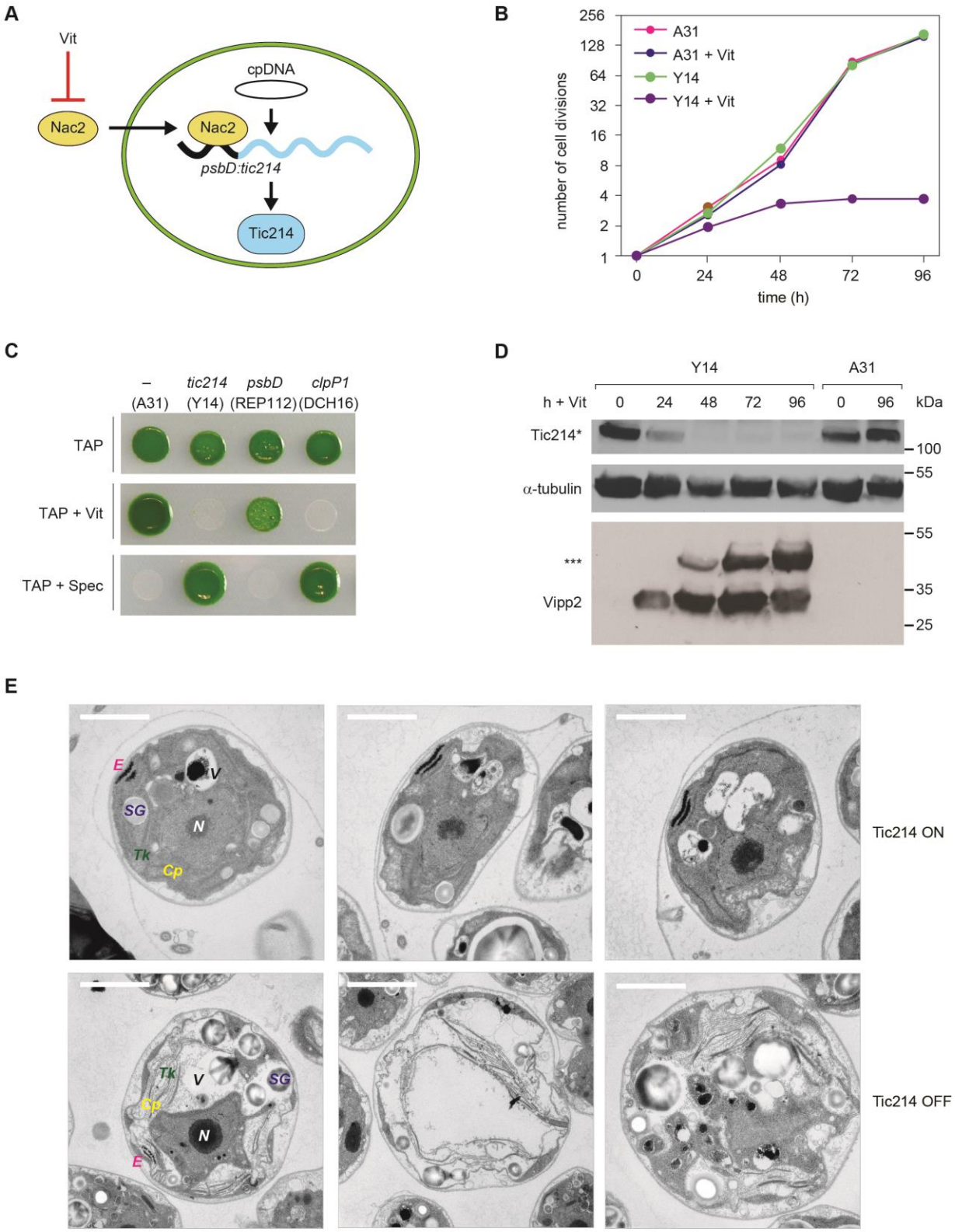

Fig. 6. Conditional depletion of Tic214 inhibits cell growth.
(*A*) Schematic illustration of selective Vit-mediated Tic214 depletion in Y14 cells. The Nac2 protein is translated in the cytosol and imported into the chloroplast, where it is required for expression of the chimeric *psbD:tic214* transgene. Accumulation of the Nac2 protein, and in turn of Tic214, is down-regulated upon the addition of thiamine and vitamin B_{12} to the growth media ("Vit").
(*B*) Growth curve of Y14 and the A31 control strains in TAP without or with Vit (20 μg /L vitamin B_{12} and 200 μM thiamine HCl) under standard light conditions (~60 μmol $m^{-2}s^{-1}$ irradiance).
(*C*) Growth of A31, Y14, REP112 and DCH16 strains was tested by spotting cells on plates containing acetate (TAP) with and without Vit (20 μg/L vitamin B_{12} and 200 μM thiamine HCl) and in TAP supplied with 100 μg/ml spectinomycin (Spec) on which only chloroplast transformants can survive. The chloroplast gene controlled by Nac2 in each strain is indicated at the top. A31 is used as a control, since no chloroplast transcript is under the control of the Vit-mediated Nac2 expression in this strain. Expression of the chimeric *psbD:tic214* gene is repressed by Vit in Y14, expression of the endogenous *psbD* is repressed by Vit in REP112 whereas the chimeric *psbD:clpP1* is repressed by Vit in DCH16 (*70, 71*).
(*D*) Immunoblot analysis of Tic214 and Vipp2 in Y14 and A31 treated with Vit for the indicated times. The three asterisk indicate a potential SDS-resistant Vipp2 aggregate. Tic214* denotes the 110 kDa protein band detected by the Tic214 antibody. α-tubulin was used as a loading control.
(*E*) Electron microscopy of Y14 cells supplemented with Vit for 96 hours (lower row, "Tic214 OFF"). The control cells without Vit treatment ("Tic214 ON") are shown in the upper row (scale bar = 2 μm). Intracellular compartments are labeled as follows: *Cp* = chloroplast; *Tk* = thylakoids; *E* = eyespot; *SG* = starch granules; *V* = vacuole; *N* = nucleus.

Figure 7

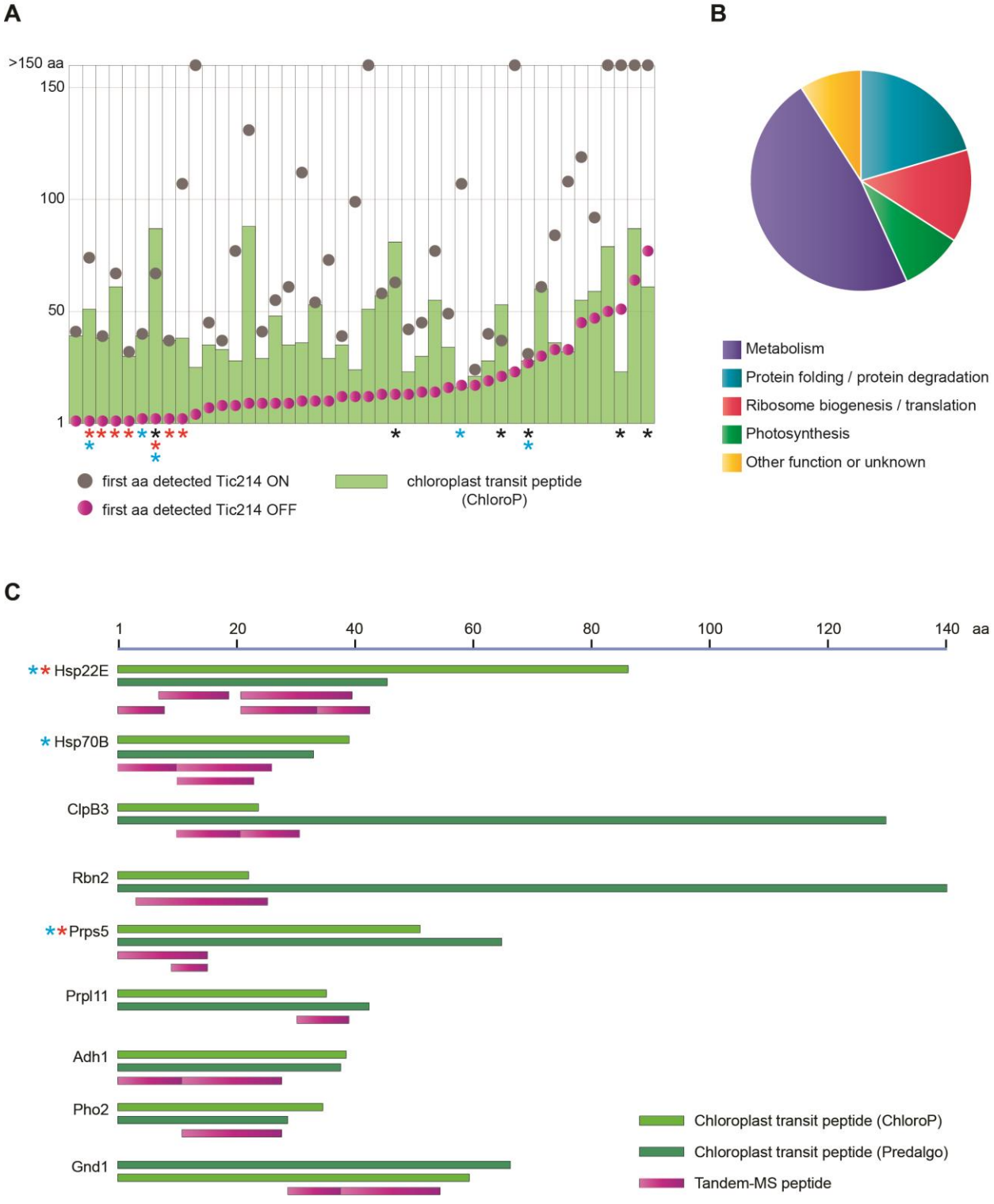

Fig. 7. Detection of chloroplast precursor proteins upon Tic214 depletion.
(*A*) Schematic representation of the 44 proteins (listed in *SI Appendix*, Table S11) for which one or more peptide covering the putative chloroplast transit peptide (cTP) could be detected, selectively upon Tic214 depletion. The green bar indicates the length of the cTP (i.e. number of amino acids) as predicted by ChloroP (*96*). The circles indicate the first amino acid position of the most N-terminal MS-peptide detected in the presence (grey) or absence (magenta) of Tic214. The black asterisks indicate those cases when peptides containing precursor sequences were observed only according to the cTP length predicted by Predalgo (*65*). The red and light blue asterisks indicate proteins that have an acetylation on their N-terminal methionine and are ubiquitylated upon Tic214 repression, respectively.
(*B*) Pie-chart summarizing the functional classification of the proteins shown in A. Metabolism (n=21); Protein folding / Protein degradation (n=9); Ribosome biogenesis / translation (n=6); Photosynthesis (n=4); Other functions or unknown (n=4).
(*C*) The location and length of peptides spanning the cTP are depicted for some of the proteins shown in A. The light and dark green bars indicate the cTP length as predicted by ChloroP and Predalgo, respectively. The magenta bars indicate the length of each MS-peptide, selectively detected upon Tic214 depletion.

Table 1

Spectral counts for proteins co-immunoprecipitated with Tic20 and Tic214. Tic214* denotes the 110 kDa protein band detected by the Tic214 antibody. The newly identified chloroplast translocon associated proteins (Ctap) are highlighted in bold. Tic214 interacting partners were eluated under denaturing conditions and gel regions corresponding to the antibody chains were excluded during HPLC-MS/MS analysis. The asterisks (**) indicate those proteins that escaped detection because of their co-migration with the antibody chains.

		Co-IP with Tic20			Co-IP with Tic214	
		Spectral counts			Spectral counts	
Gene ID	**Protein ID**	**Tic20**	**mock**	**rank**	**Tic214**	**mock**
	Protein import					
tic214 (orf1995)	Tic214/Tic214*	543	< 1	1st	305	< 1
Cre06.g300550	Tic100	335	< 1	2nd	357	< 1
Cre03.g175200	Toc75	228	< 1	3rd	260	< 1
Cre16.g696000	**Ctap2**	88	< 1	8th	317	< 1
Cre17.g734300	Toc90	160	< 1	5th	193	< 1
Cre08.g379650	Tic20	186	< 1	4th	< 1**	< 1
Cre17.g727100	Tic56	50	< 1	11th	1**	< 1
Cre06.g252200	Toc34	68	< 1	9th	17	< 1
Cre17.g707500	Toc120	7	< 1	142th	35	< 1
Cre10.g452450	Tic110	8	< 1	131th	15	< 1
	AAA proteins					
Cre07.g352350	Fhl3	39	< 1	14th	71	< 1
Cre03.g201100	Fhl1	22	< 1	37th	71	< 1
Cre17.g739752	**Ctap1**	14	< 1	62th	37	< 1
	Translation					
Cre16.g659950	Prps5	22	< 1	35th	38	2
orf712	Rps3-like	27	< 1	33st	20	< 1
	Unknown		< 1			< 1
Cre12.g532100	**Ctap3**	127	< 1	6th	18	< 1
Cre17.g722750	**Ctap4**	112	< 1	7th	12	< 1
Cre03.g164700	**Ctap5**	67	< 1	10th	10	< 1
Cre04.g217800	**Ctap6**	12	< 1	80nd	19	< 1
Cre08.g378750	**Ctap7**	8	< 1	123th	39	< 1
	Photoreception					
Cre01.g002500	Chlamyopsin	13	< 1	65th	5	2

Table 2

Spectral counts for proteins associated with pre-Fdx1 translocation intermediates. The three asterisks (***) indicate genes co-expressed with *TIC20*. Tic214* denotes the 110 kDa protein band detected by the Tic214 antibody.

		Spectral counts					
Gene ID	**Protein ID**	**mock**		**no ATP**		**0.3 mM ATP**	
*tic214 (orf1995)****	Tic214/Tic214*	0	0	2	0	98	74
Cre16.g696000***	Ctap2	1	0	8	1	96	87
Cre03.g175200***	Toc75	0	0	1	1	57	46
Cre17.g734300***	Toc90	0	0	3	0	56	46
Cre17.g722750***	Ctap4	0	0	1	0	35	27
Cre12.g532100***	Ctap3	0	0	0	0	23	18
Cre06.g300550***	Tic100	0	0	0	0	22	15
Cre01.g049900	Not annotated	0	0	0	0	20	12
Cre06.g252200***	Toc34	0	1	1	1	19	17
Cre03.g164700***	Ctap5	0	0	1	0	17	17
Cre09.g416800	Not annotated	0	0	1	0	14	12
Cre12.g527550	Not annotated	0	0	0	0	14	10
Cre01.g002500	Chlamyopsin	0	0	0	0	10	10
Cre07.g352350***	Fhl3	0	0	0	0	10	8
Cre09.g402100	Not annotated	0	0	0	0	8	5
Cre17.g727100***	Tic56	0	0	0	0	8	7
Cre08.g378750***	Ctap7	0	0	0	0	4	6
Cre03.g173000	Not annotated	0	0	0	0	4	6

Figure S1

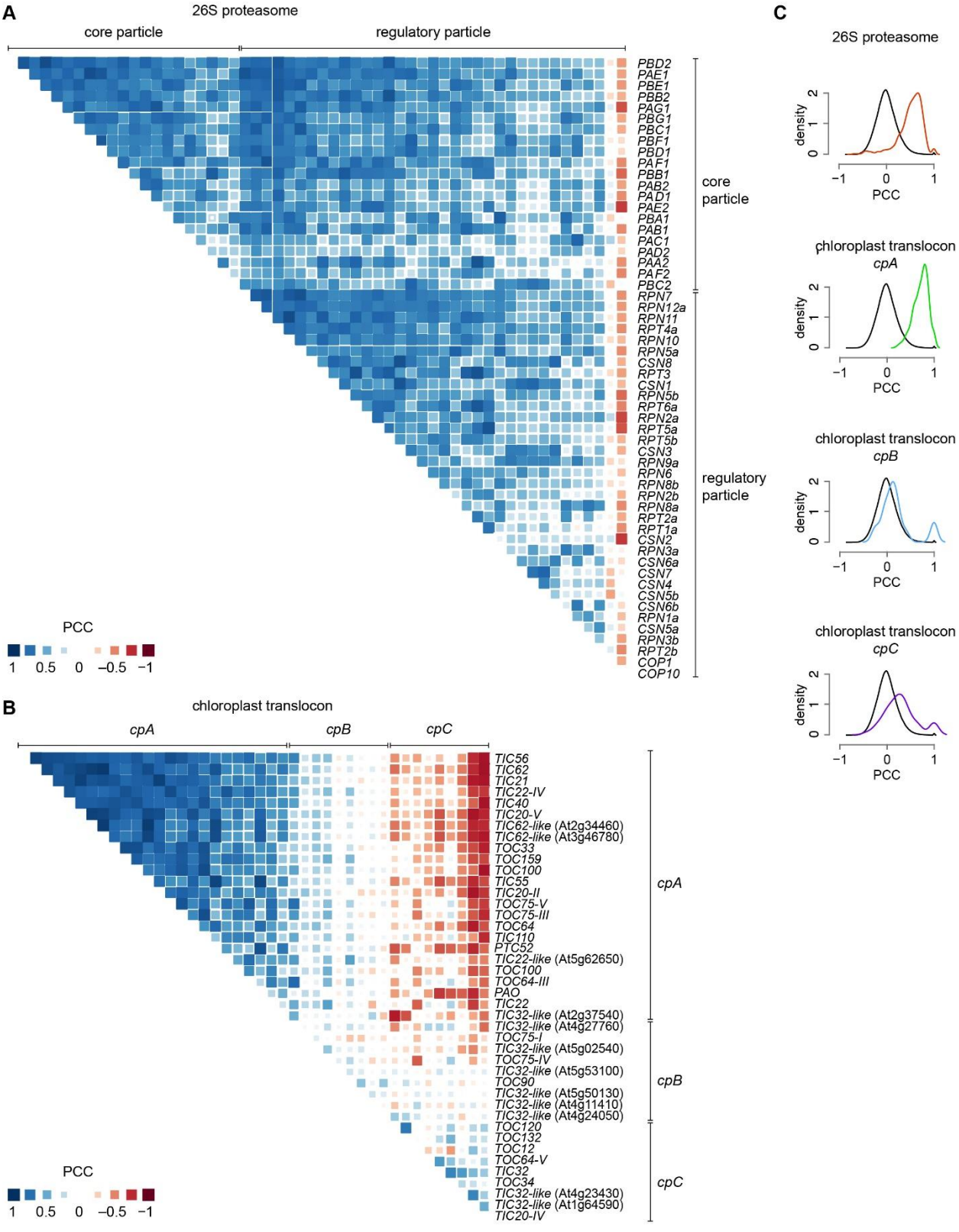

Fig. S1. Co-expression patterns of Arabidopsis genes encoding components of the plastid translocon.

(*A*) Correlation matrix for Arabidopsis genes encoding subunits of the 26S proteasome (listed in *SI Appendix*, Table S5).

(*B*) Correlation matrix for Arabidopsis genes encoding components of the chloroplast translocon (listed in *SI Appendix*, Table S5), clustered in three sub-groups: *cpA*, *cpB,* and *cpC*.

(*C*) PCC distribution for all gene pairs encoding core and regulatory particles of the 26S proteasome (red line), for all gene pairs encoding chloroplast translocon components as a function of their subgroup — *cpA* (green line), c*pB* (blue line) and *cpC* (purple line) — and for all gene pairs in the genome (black line) used as a negative control. Statistical significance of all distributions was tested by Kolmogorov-Smirnov test, comparing each sets of PCC values with a randomly generated normal distribution of equal element number. The results of this analysis are available in *SI Appendix*, Table S4.

Figure S2

Figure S2 (continuation)

Figure S2 (continuation)

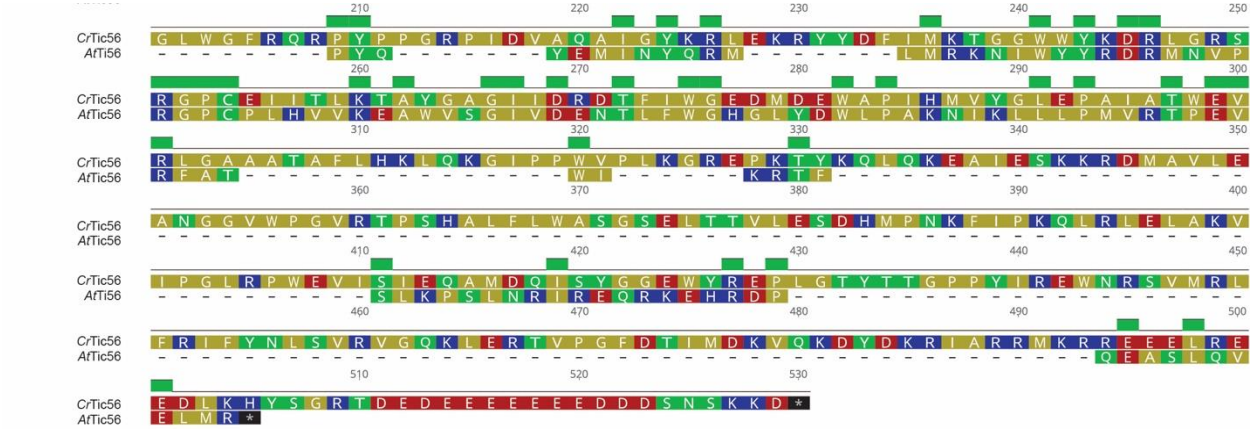

C

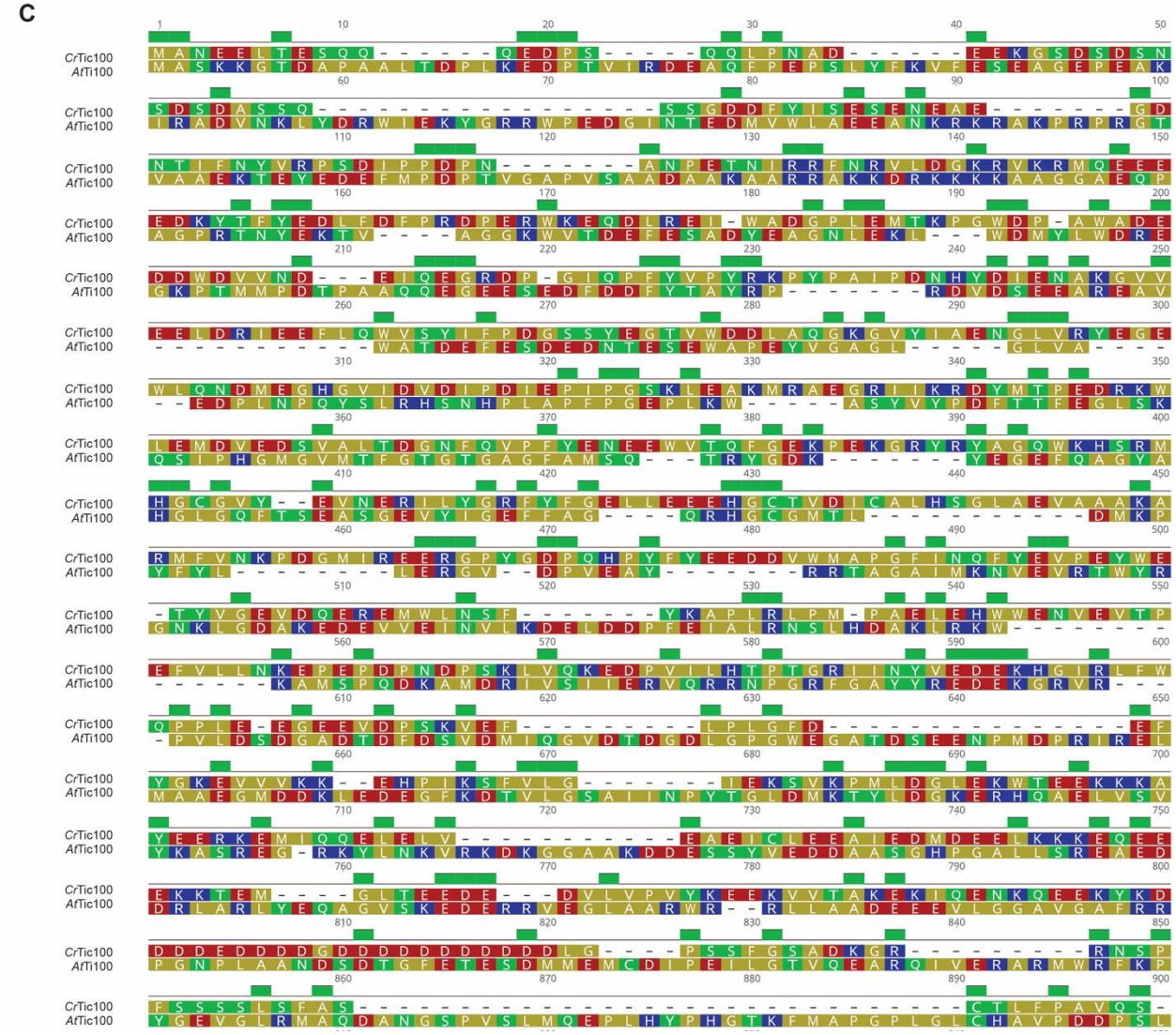

Figure S2 (continuation)

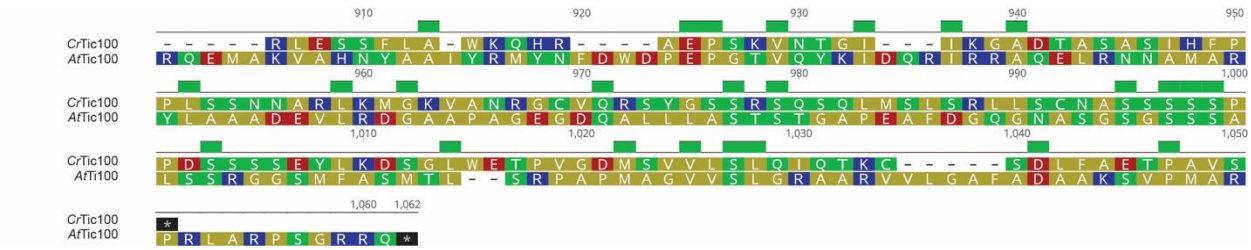

Fig. S2. Sequence comparison of TIC components of Chlamydomonas and Arabidopsis.

All protein alignments were performed using Geneious 11.1.5 (alignment method: MUSCLE, Topology: LINEAR). The amino acids were colored according to their polarity as follows: Yellow = Non-polar (G, A, V, L, I, F, W, M, P), Green = Polar, uncharged (S, T, C, Y, N, Q), Red = Polar, acidic (D, E), Blue = Polar, basic (K, R, H).

(*A*) Tic214 sequence comparison of Arabidopsis and Chlamydomonas (*orf1995*/*ycf1*). Identity = 321/2102 (15%), Positives = 715/2102 (34%), Gaps = 423/2102 (20%).

(*B*) Tic56 sequence comparison of Arabidopsis and Chlamydomonas (At5g01590/Cre17.g727100). Identity = 71/530 (13%), Positives = 120/530 (22%), Gaps = 287/530 (54%).

(*C*) Tic100 sequence comparison of Arabidopsis and Chlamydomonas (At5g22640/Cre06.g300550). Identity = 179/1062 (16%), Positives = 321/1062 (30%), Gaps = 296/1062 (27%).

Figure S3

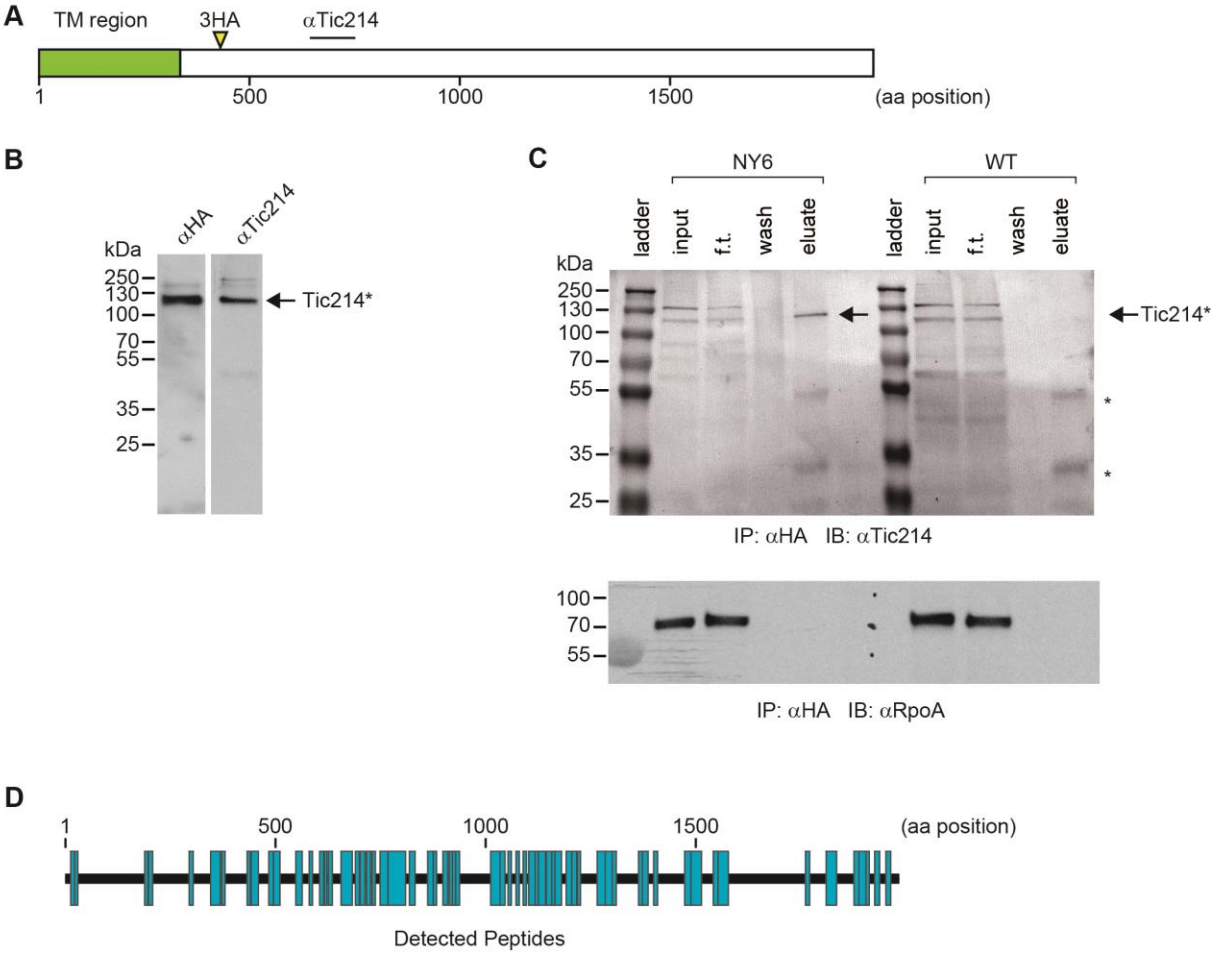

Fig. S3:
Characterization of Tic214.
(*A*) Organization of Tic214 with 8 N-terminal transmembrane domains and the remaining basic region. The region used for purifying a recombinant protein and producing antibodies (αTic214) and the insertion site of the HA-epitope after T402 (3XHA), are indicated.
(*B*) Immunoblot analysis of total protein of NY6 cells containing HA-tagged Tic214 with anti-HA and anti-Tic214 antibodies. Tic214* denotes the 110 kDa protein band detected by the Tic214 antibody.
(*C*) Co-immunoprecipitation of total protein from NY6 containing HA-tagged Tic214. Cellular extracts from NY6 and wild type (WT) were incubated with an affinity matrix containing HA antibodies. After extensive washing of the matrix, bound proteins were eluted with SDS buffer and immunoblotted with HA antiserum. The black arrows highlight the position of the 110 kDa protein band detected by the Tic214 antibody in the immunoblot.
(*D*) The entire *tic214* mRNA is translated as a protein of 232 kDa. After immunoprecipitation with anti-HA antibodies, proteins were digested with trypsin and

analyzed by mass spectrometry. The distribution of the identified peptides of Tic214 (indicated in blue) over the entire Tic214 sequence (between D15 and K1979) is drawn to scale.

Figure S4

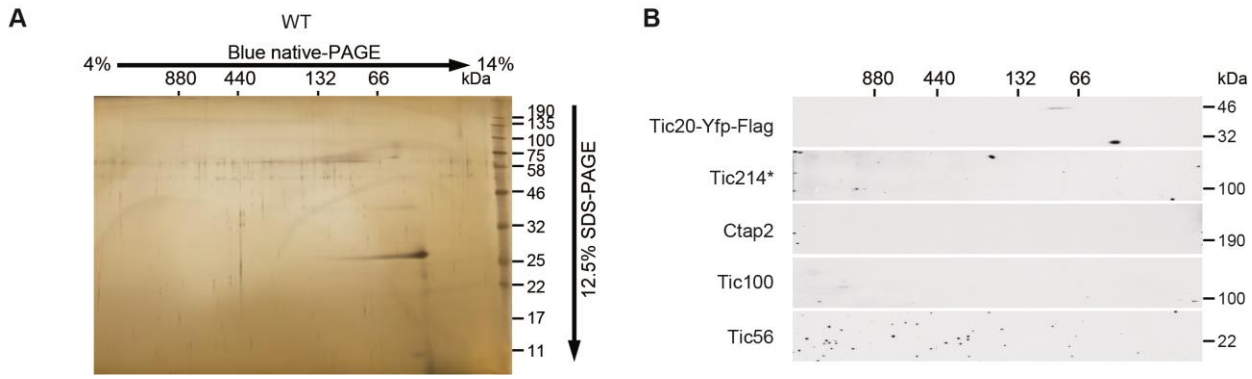

Fig. S4. 2D blue native/SDS-PAGE separation of a mock purified sample.
(*A*) A mock purified sample with untagged Tic20 was analyzed as in Fig. 4A.
(*B*) A mock purified sample with untagged Tic20 was analyzed as in Fig. 4B.

Figure S5

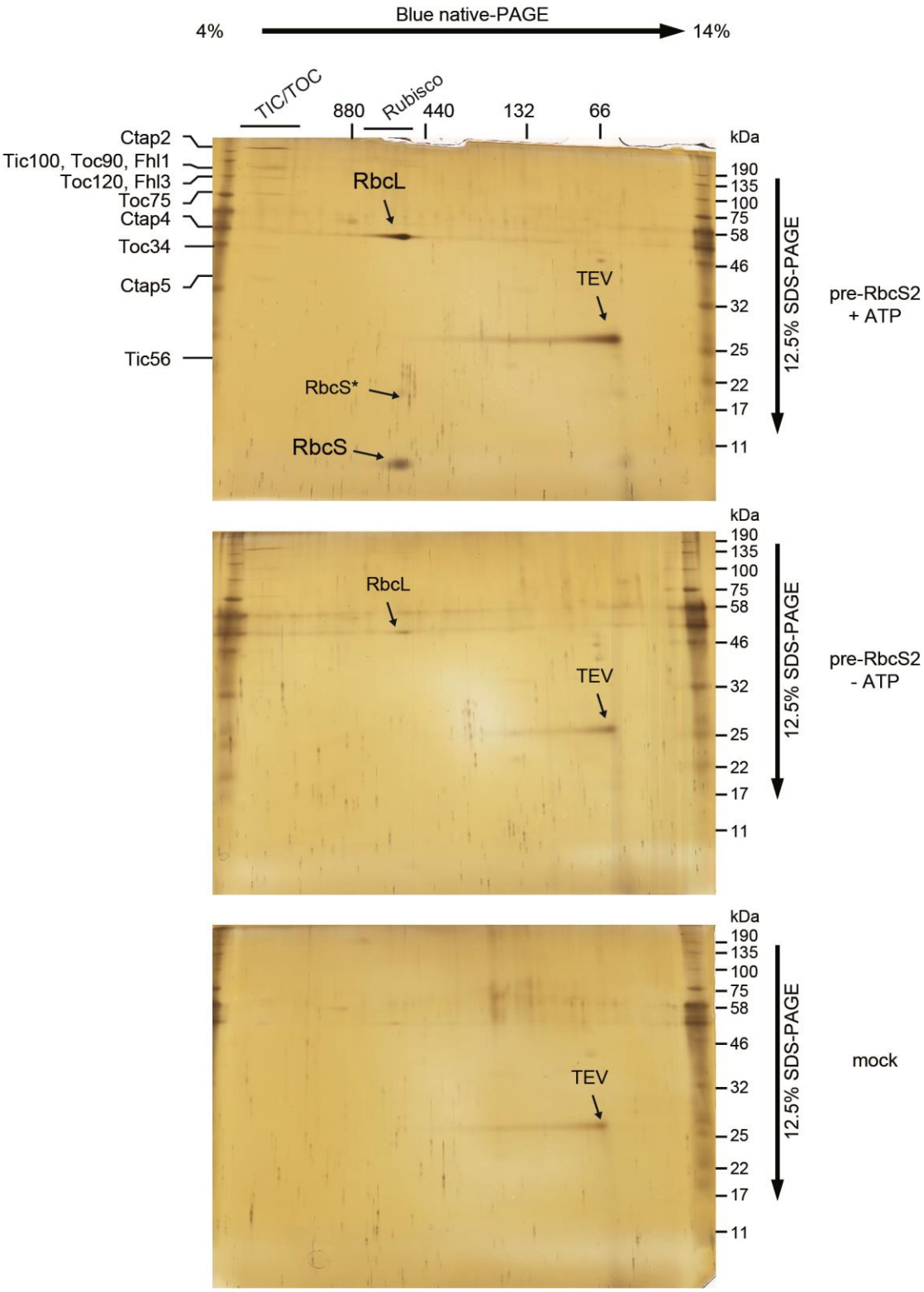

Fig. S5. 2D blue native/SDS-PAGE analysis of purified translocation intermediates. The pre-RbcS2 was used for in vitro import experiments with Chlamydomonas chloroplasts in the presence or absence of ATP. Translocation intermediates were purified and analyzed by 2D blue native/SDS-PAGE separation followed by silver staining. Mock-purified samples prepared from the same amounts of chloroplasts without the addition of pre-proteins were also analyzed. Bands containing proteins identified by mass spectrometry are labeled.

Figure S6

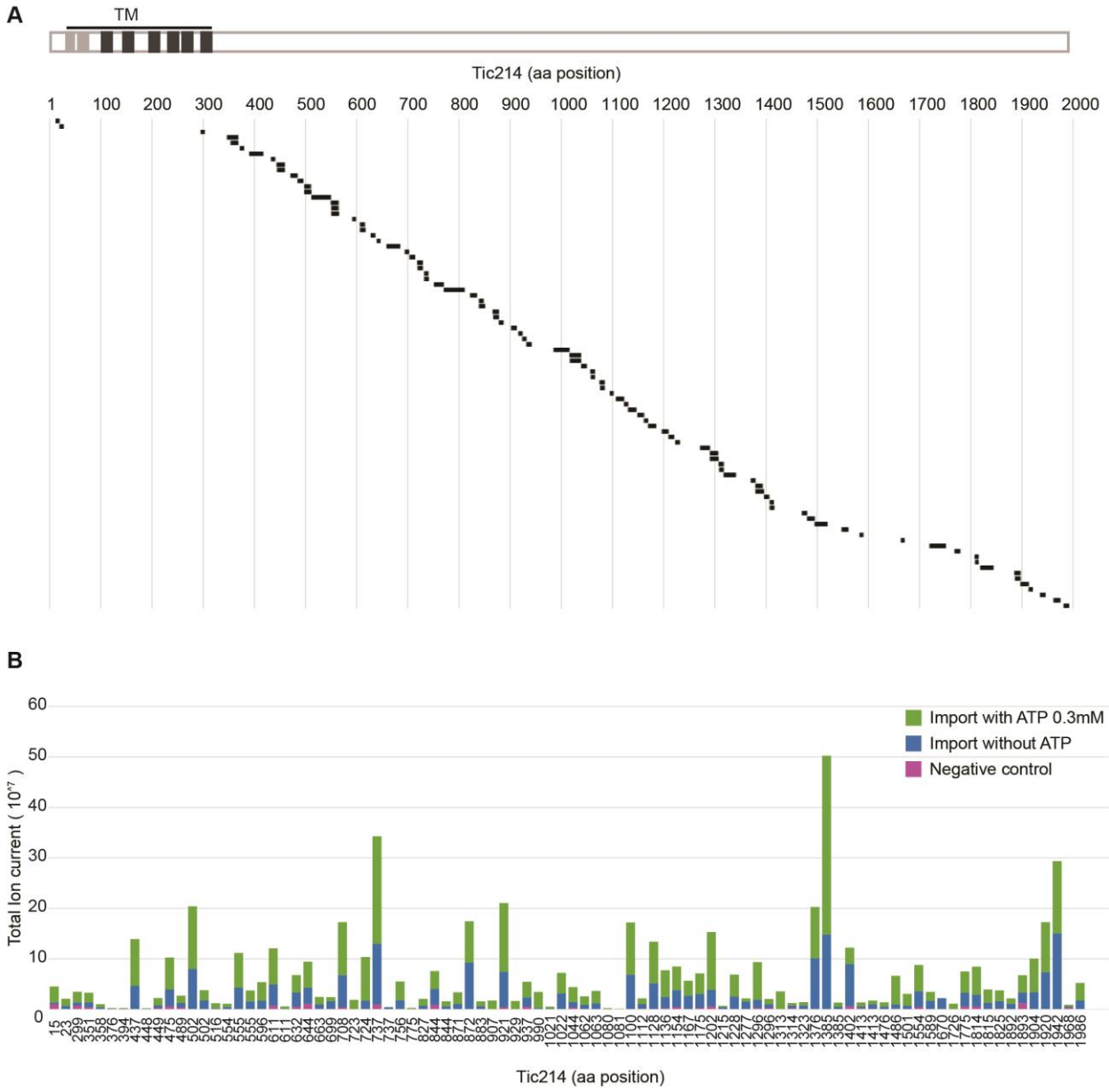

Fig. S6. Distribution of Tic214-derived peptides identified by LC-MS/MS analysis of the translocation intermediates.

(*A*) (*upper panel*) Strongly and weakly predicted transmembrane domains in Tic214 protein are shown in dark and light grey, respectively. (*lower panel*) Tic214-derived peptides identified upon mass spec analysis of translocation intermediates are indicated as dark bars along the length of the protein.

(*B*) ATP-dependent association of Tic214 with translocating pre-proteins is shown as measured by total ion current detected for Tic214-derived peptides. The numbers of the

starting amino acids of the identified peptides in full-length Tic214 are shown below the horizontal axis. In the negative control, no pre-protein was added to the chloroplasts.

Figure S7

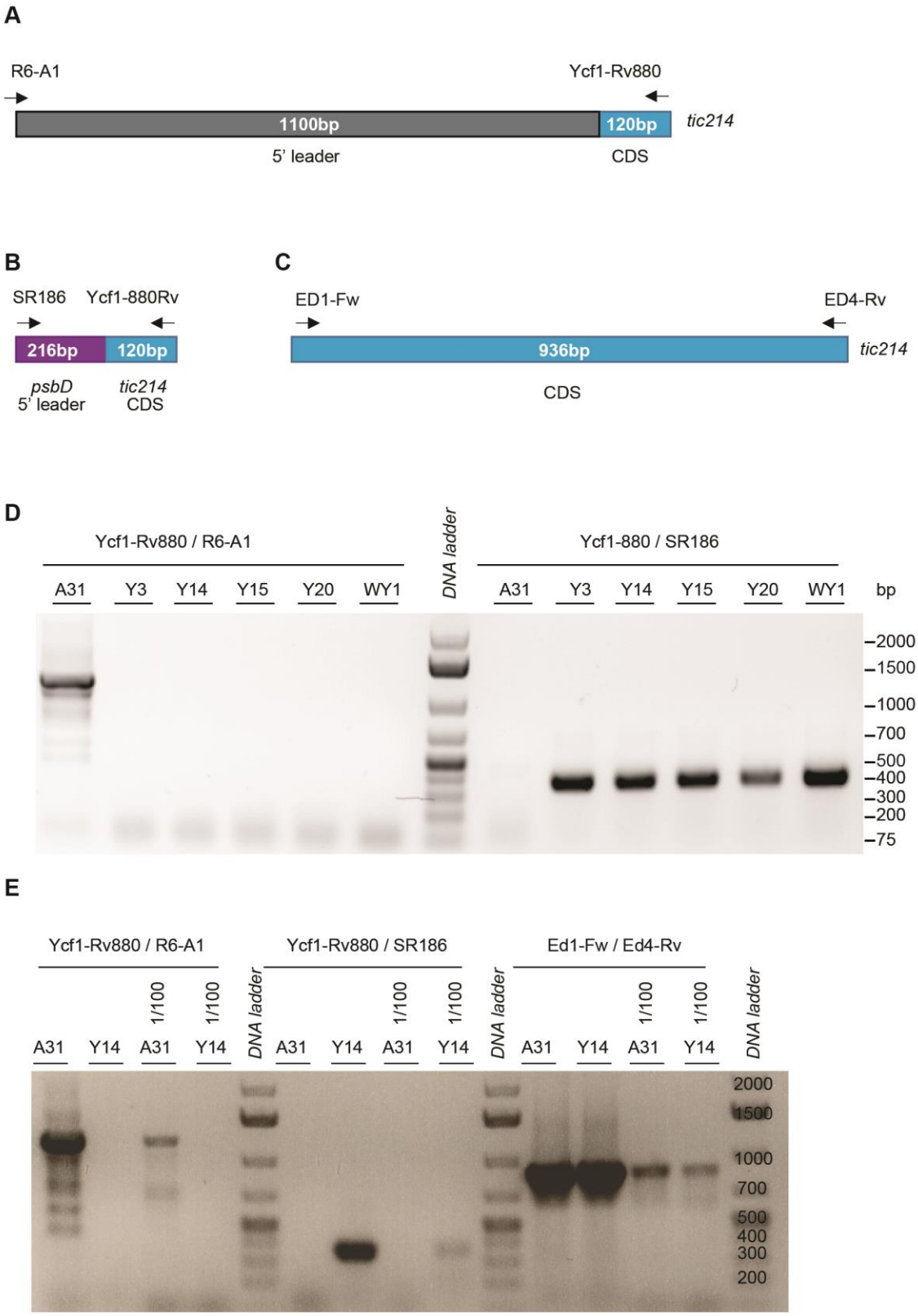

Fig. S7. Homoplasmicity of the Y14 strain.
(*A*) Location of primers used for PCR on authentic *tic214 (orf1995)* leader and coding sequence (CDS).
(*B*) Location of primers used for PCR on chimeric *psbD*:*tic214* gene.
(*C*) Location of primers used for PCR on *tic214* CDS.
(*D*) Y strains were obtained by transformation of A31 with the pRAM73.19 plasmid containing the *psbD* 5' leader fused to the CDS of *tic214* and the *aadA* spectinomycin resistance cassette. The WY1 strain was obtained in the same way except that the wild-type cell line was used for transformation. The authentic *tic214* locus was examined by PCR using the primers shown in panel A, while the chimeric *psbD*5'UTR:*tic214* was analyzed by PCR using primers shown in panel B.
(*E*) The same PCR reactions shown in panel D were repeated for A31 and Y14. In this case, a 1/100 dilution of the genomic DNA was also tested to make sure that at least one gene copy per chloroplast is detectable as there are ~80 copies of chloroplast DNA molecules per chloroplast in Chlamydomonas. Primers shown in panel C (spanning a region of *tic214* CDS) were used as loading control.

Figure S8

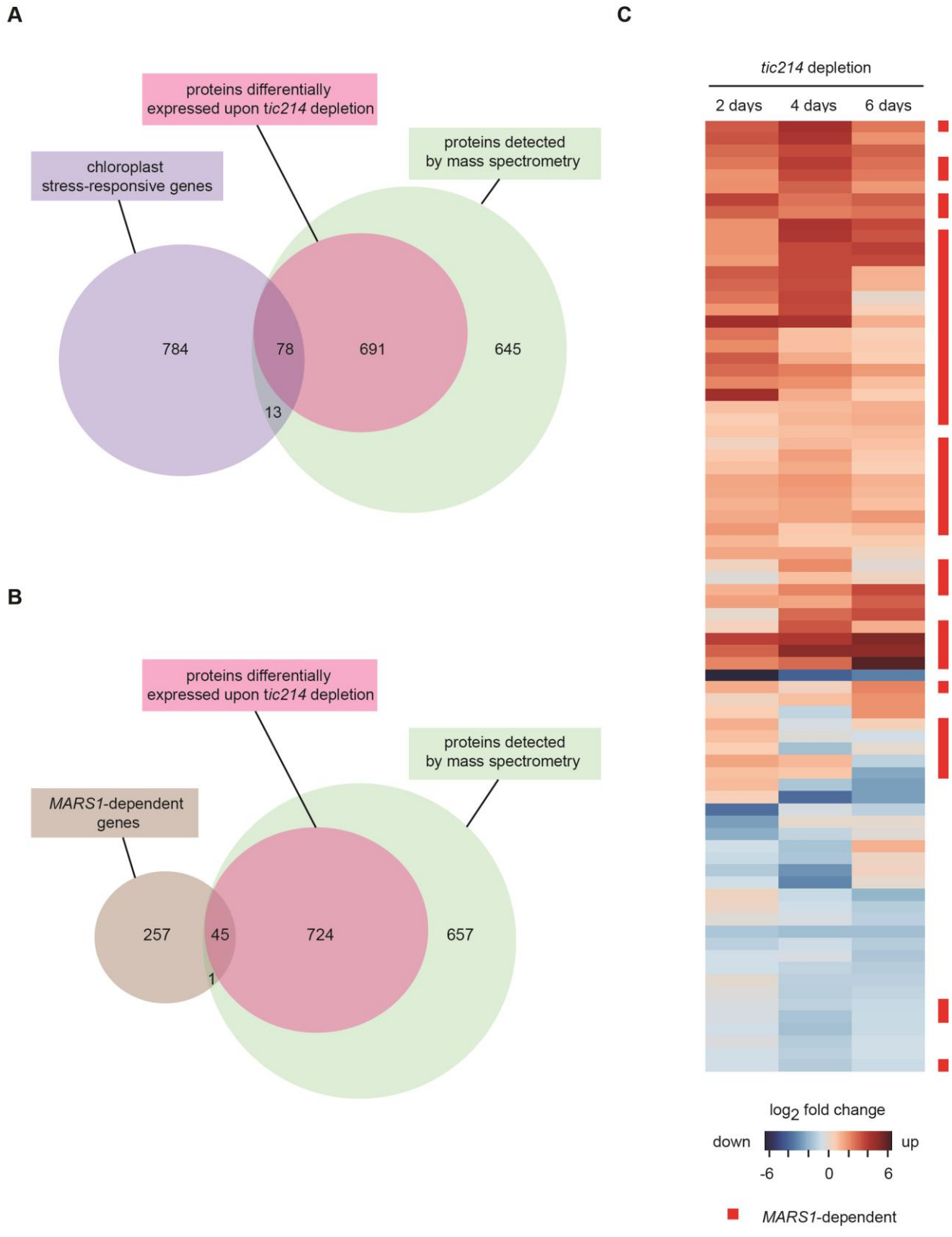

Fig. S8. Chloroplast-stress responsive proteins differentially expressed upon Tic214 depletion.

(*A*) Venn diagram highlighting the number of chloroplast stress-responsive proteins that could be detected by mass spectrometry (n = 91). About 80% (n = 78) were also differentially expressed upon *tic214* depletion (Protein IDs are listed in *SI Appendix*, Table S13). Chloroplast stress-responsive proteins are defined as proteins encoded by nuclear genes differentially expressed upon down-regulation of the chloroplast Clp protease and in response to excessive light in Chlamydomonas cells (*75*).

(*B*) Venn diagram highlighting the number of proteins encoded by *MARS1*-dependent genes and detected by mass spectrometry (n = 46). Over 95% (n = 45) were differentially accumulated upon *tic214* depletion (Protein IDs are listed in *SI Appendix*, Table S13). *MARS1* encodes a critical component of the chloroplast unfolded protein response (*75*).

(*C*) Heatmap showing the proteins encoded by chloroplast stress-responsive genes and differentially accumulated upon *tic214* depletion. The red squares on the side indicate those proteins encoded by *MARS1*-dependent genes.

Table S1

Arabidopsis components of the TOC complex and their putative Chlamydomonas orthologs from BLAST analysis.

Arabidopsis			Chlamydomonas			BLAST	
Gene ID	**Protein name**	**Protein length (aa)**	**Gene ID**	**Protein name**	**Protein length (aa)**	**Score**	**p-value**
At5g05000	Toc33	313	Cre06.g252200	Toc33/34	397	150.2	1.60E-41
			Cre17.g734300	Toc90	967	62.8	7.60E-11
			Cre17.g707500	Toc120	1080	58.2	2.70E-09
At1g02280	Toc34	297	Cre06.g252200	Toc33/34	397	145.6	1.50E-39
			Cre17.g734300	Toc90	967	67	3.60E-12
			Cre17.g707500	Toc120	1080	55.1	3.60E-08
At1g08980	Toc64	425	Cre11.g467630	Toc64	540	318.9	3.50E-103
At3g17970		589	Cre11.g467630			250.8	3.40E-75
At5g09420		603	Cre11.g467630			226.1	6.10E-66
At3g46740	Toc75-III	818	Cre03.g175200	Toc75	798	303.9	8.80E-90
At4g09080	Toc75-IV	396	Cre03.g175200			222.2	2.30E-64
At5g19620	Toc75-V	732	Cre09.g388097	Oep80	651	443	6.40E-145
At5g20300	Toc90	793	Cre17.g734300	Toc90	967	163.3	2.60E-41
At4g15810	Toc100	918	Cre17.g734300	Toc90	967	49.7	9.70E-06
At3g16620	Toc120	1089	Cre17.g707500	Toc120	1080	172.6	1.50E-43
At2g16640	Toc132	1206	Cre17.g707500	Toc120	1080	171	6.00E-43
At4g02510	Toc159	1503	Cre17.g707500	Toc120	1080	153.7	2.00E-37

Table S2

Proposed Arabidopsis components of the TIC complex and their putative Chlamydomonas orthologs from BLAST analysis.

Arabidopsis			Chlamydomonas			BLAST	
Gene ID	**Protein name**	**Protein length (aa)**	**Gene ID**	**Protein name**	**Protein length (aa)**	**Score**	**p-value**
At1g04940	Tic20-I	274	Cre08.g379650	Tic20-I	259	68.9	1E-13
At2g47840	Tic20-II	208	Cre01.g039150	Tic20-II	185	140.6	5.8E-41
At4g03320	Tic20-IV	284	Cre08.g379650		259	51.2	2E-07
At5g55710	Tic20-V	209	Cre01.g039150	Tic20-II	185	126.7	1.2E-35
			Cre04.g225050	Tic20-III	228	125.2	1.5E-34
At2g15290	Tic21	296	Cre10.g454734[1]	Tic21a	869	152.9	4.9E-41
			Cre11.g467759	Tic21b	296	80.1	2.3E-17
At3g23710	Tic22-III	313	Cre14.g625750	Tic22	332	120.2	6.6E-31
At4g33350	Tic22-IV	268	Cre14.g625750	Tic22	332	98.6	1.1E-23
At4g23420	Tic32	333	Cre12.g556750		473	192.2	4.1E-56
			Cre09.g398252		334	168.3	2.5E-48
			Cre12.g556802		287	164.9	1.7E-47
			Cre16.g685400		355	118.6	4.9E-30
			Cre02.g113652		320	116.3	2.1E-29
At5g16620	Tic40	447	Cre12.g508000	Tic40-I	412	157.1	1.7E-42
			Cre12.g490650	Tic40-II	332	68.6	1.5E-12
At2g24820	Tic55	539	Cre06.g278245*	Pao5	564	148.3	2.8E-38
			Cre06.g305650	Pao6	766	139	1.1E-34
			Cre10.g450550	Pao3	612	137.5	1.6E-34
			Cre17.g724600	Pao2	530	134.4	7.8E-34
			Cre17.g724700	Pao1	522	129.8	3.6E-32
			Cre01.g043350	Cao	645	124	8.6E-30
			Cre03.g173450	Pao4	692	109.4	5.3E-25
			Cre11.g476500	Pao7	715	104	3.1E-23
At3g44880	Pao	537	Cre17.g724600	Pao2	530	231.1	7.6E-68
			Cre06.g278245*	Pao5	564	221.9	3.5E-64
			Cre17.g724700	Pao1	522	214.9	5.8E-62
			Cre10.g450550	Pao3	612	205.7	5.9E-58
			Cre06.g305650	Pao6	766	183.3	1.4E-49
			Cre03.g173450	Pao4	692	132.1	1.9E-32
			Cre13.g583050	Pao8	781	126.7	1.4E-30
			Cre11.g476500	Pao7	715	114	1.8E-26
At3g18890	Tic62	641	Cre06.g269050	Tic62	898	224.6	1.6E-62
			Cre07.g349700	Tic62-II	278	137.5	6.3E-36
			Cre11.g467755	Tic62-III	310	120.2	1.4E-29
			Cre03.g181250	Tic62-IV	301	105.5	1.2E-24

At2g34460	Tic62-like	280	Cre11.g467755	Tic62-III	310	212.6	2.5E-66
At1g06950	Tic110	1016	Cre10.g452450	Tic110	1046	417.2	1.6E-127
At5g01590	Tic56	527	Cre17.g727100				
At5g22640	Tic100	871	Cre06.g300550				
ycf1	Tic214 (Ycf1)	1786	*orf1995*				

[1] The current gene model appears to be a fusion of a Tic21-like gene at the 5' end and a chlorophyll a/b binding gene at the 3' end.

[*] This gene is annotated as PAO-like in Phytozome, and is one of 8 putative Chlamydomonas homologs. All other PAO-like genes were assigned a number (from 1-4 and 6-8). Hence, we refer to the protein encoded by this gene as Pao5, although the annotation does not reflect the gene number.

Table S8

Genes co-expressed with Chlamydomonas *TIC20*.

Gene ID	Mutual rank	Protein Name (Annotation)
Cre06.g300550 [a,b]	8	Tic100
Cre16.g696000 [a,b]	3	Ctap2
Cre17.g727100 [b]	6	Tic56
Cre07.g352350 [b]	10	Fhl3
Cre03.g201100 [b]	6	Fhl1
Cre17.g739752 [b]	47	Ctap1
Cre12.g532100 [b]	9	Ctap3
Cre17.g722750 [b]	19	Ctap4
Cre03.g164700 [b]	22	Ctap5
Cre08.g378750 [b]	21	Ctap7
Cre03.g175200 [a,b]	5	Toc75
Cre17.g734300 [a,b]	4	Toc90
Cre08.g379650 [a,b]	1	Tic20
Cre06.g252200 [a,b]	21	Toc34
Cre02.g080250	4	Ylmg1 (YGGT family)
Cre13.g573900	6	Nss3 (Sodium/solute transporter)
Cre03.g201750	6	not annotated
Cre12.g527550	8	not annotated
Cre10.g451900	10	Ths1 (Threonine synthase)
Cre13.g604650	11	Metallopeptidase family M24
Cre16.g683081	11	Sec-C motif domain-containing protein
Cre12.g497850	12	not annotated
Cre08.g365600	12	Hydroxymethylpyrimidine kinase
Cre09.g386200	12	Opr36
Cre02.g142246	13	not annotated
Cre04.g216950	15	KasIII (Beta-ketoacyl-[acyl-carrier-protein] synthase III)
Cre03.g160500	16	Tsk1 (Lysine-tRNA ligase)
Cre16.g659850	16	Cgl37 (Shikimate kinase-related protein)
Cre16.g663150	17	Thiosulfate sulfurtransferase
Cre03.g171100	17	not annotated
Cre01.g052250	17	Trx1 (Thioredoxin x)
Cre04.g214501	18	Pnp1 (Polynucleotide phosphorylase)
Cre16.g691000	19	Efp1 (Organellar elongation factor P)
Cre12.g552850	19	Cgl77
Cre09.g403145	20	not annotated
Cre17.g747297	20	peptidyl-tRNA hydrolase
Cre14.g629650	21	Nik1 (Nickel transporter)
Cre05.g240850	23	ThiC (Hydroxymethylpyrimidine phosphate synthase)
Cre09.g405150	24	Pus1 (tRNA-pseudouridine synthase)

[a] gene is part of the plastid translocon based on our BLAST analysis (SI Appendix, Tables S1 and S2)

[b] encoded protein was identified during the co-immunoprecipitation studies presented in this manuscript.

Table S12

Putative Arabidopsis orthologs of chloroplast protein precursors detected upon depletion of Tic214 in Chlamydomonas.

Chlamydomonas		Arabidopsis		
Gene ID	Gene Name	Ortholog Gene ID	Ortholog Gene Name	Ortholog Relationship
Cre03.g144707		At1g70820		one-to-one
Cre03.g146187		At2g19940		one-to-one
Cre03.g189800		At3g01480	*CYP38*	one-to-one
Cre06.g273700		At5g23120	*HCF136*	one-to-one
Cre06.g282000	*STA3*	At1g11720	*SS3*	one-to-one
Cre06.g284750		At1g18070		one-to-one
Cre08.g364800		At1g74260	*PUR4*	one-to-one
Cre09.g411200	*TEF5*	At1g71500		one-to-one
Cre10.g433000		At3g48110	*EDD1*	one-to-one
Cre11.g481500		At4g26900	*AT-HF*	one-to-one
Cre12.g497300	*CAS1*	At5g23060	*CaS*	one-to-one
Cre12.g500650	*RNB2*	At5g02250	*EMB2730*	one-to-one
Cre16.g663900	*PBGD1*	At5g08280	*HEMC*	one-to-one
Cre17.g719900	*PWD1*	At5g26570	*PWD*	one-to-one
Cre48.g761197		At2g43030		one-to-one
Cre01.g061077		At1g16880		one-to-many
Cre01.g061077		At5g04740		one-to-many
Cre02.g080200	*TRK1*	At2g45290		one-to-many
Cre02.g080200	*TRK1*	At3g60750		one-to-many
Cre02.g090850	*CLPB3*	At2g25140	*CLPB4*	one-to-many
Cre02.g090850	*CLPB3*	At5g15450	*CLPB3*	one-to-many
Cre03.g158000		At3g48730	*GSA2*	one-to-many
Cre03.g158000		At5g63570	*GSA1*	one-to-many
Cre03.g181300		At1g48860		one-to-many
Cre03.g181300		At2g45300		one-to-many
Cre05.g234638		At2g16570	*ASE1*	one-to-many
Cre05.g234638		At4g34740	*ASE2*	one-to-many
Cre05.g234638		At4g38880	*ASE3*	one-to-many
Cre06.g250100	*HSP70B*	At4g24280	*cpHsc70-1*	one-to-many
Cre06.g250100	*HSP70B*	At5g49910	*cpHsc70-2*	one-to-many
Cre07.g340900		At2g28305	*LOG1*	one-to-many
Cre07.g340900		At2g35990		one-to-many
Cre07.g340900		At2g37210		one-to-many
Cre07.g340900		At3g53450		one-to-many

Cre07.g340900		At4g35190		one-to-many
Cre07.g340900		At5g03270		one-to-many
Cre07.g340900		At5g06300		one-to-many
Cre07.g340900		At5g11950		one-to-many
Cre10.g423650	*PRPL11*	At1g32990	*PRPL11*	one-to-many
Cre10.g423650	*PRPL11*	At5g51610		one-to-many
Cre12.g485800	*FTSH1*	At1g50250	*FTSH1*	one-to-many
Cre12.g485800	*FTSH1*	At5g42270	*VAR1*	one-to-many
Cre12.g526800		At1g64190		one-to-many
Cre12.g526800		At3g02360		one-to-many
Cre12.g526800		At5g41670		one-to-many
Cre12.g518900		At2g27680		many-to-one
Cre07.g339150		At1g55490	*CPN60B*	many-to-many
Cre07.g339150		At3g13470		many-to-many
Cre07.g339150		At5g56500		many-to-many
Cre12.g541800		At1g20380		many-to-many
Cre12.g541800		At1g76140		many-to-many